UNIVERSITY OF OKLAHOMA

GRADUATE COLLEGE

STAGED THERMAL FRACTIONATION OF BIOMASS FOR SEGREGATION OF HEMICELLULOSE, CELLULOSE AND LIGNIN DERIVED PRODUCTS

A THESIS

SUBMITTED TO THE GRADUATE FACULTY

in partial fulfillment of the requirements for the

Degree of

MASTER OF SCIENCE

By

RAJIV REDDY JANUPALA
Norman, Oklahoma
2016

STAGED THERMAL FRACTIONATION OF BIOMASS FOR SEGREGATION OF HEMICELLULOSE, CELLULOSE AND LIGNIN DERIVED PRODUCTS

A THESIS APPROVED FOR THE
SCHOOL OF CHEMICAL, BIOLOGICAL AND MATERIALS ENGINEERING

BY

_____
Dr. Lance Lobban, Chair

_____
Dr. Richard Mallinson

_____
Dr. Steven Crossley

Dedication

To my parents and my sister.

Thank you for your love, support, encouragement and sacrifices

Acknowledgements

I am very fortunate to have pursued my graduate college at University of Oklahoma; therefore, there are many people to thank for their part in my success. First and foremost, I would like to thank my advisor, ***Dr. Lance L. Lobban***, for his guidance and support throughout my three years in graduate school, and especially for his confidence in me. Besides my research, he has also helped me in choosing graduate classes and ensured I was performing well. His comments and questions were very beneficial in my completion of the thesis manuscript. I could not have imagined having a better advisor and mentor for my master's study.

I would also like to thank my committee members, ***Dr. Richard Mallinson*** *and* ***Dr. Steven Crossley***, for their contributions to this work. Over the years, each has given me scientific guidance, many insightful suggestions and demonstrated a sincere interest in my work.

I would like to thank my cousin brother ***Ravi Guddeti,*** who himself is a chemical engineer and has inspired me in taking chemical engineering at the undergraduate level. He has also assisted me in applying to various graduate schools for my master's study. I will always be thankful to him for his support and guidance during my three years in graduate school.

I must express my sincere gratitude to ***Christopher Waters*** for his constant support throughout the three years of my master's study. Be it graduate classes or research, he has always extended his help for me. I also thank him for inviting me to his family's Thanksgiving party and treating me to a sumptuous lunch as well as meeting me to some wonderful people.

I would like to extend my gratitude to all the undergraduate students and in particular, ***Edward Rich***, who have helped me in my research. Eddie, thank you for staying late in the evenings and coming early in the mornings to assist me conduct experiments in the lab.

I would like to thank my fellow pyrolysis group members, Shaolong Wan, Daniel Dixon, Tyler Vann and Issac Schneberger, for their friendship, help and valuable insights during group meetings.

I would like to thank my friends for their understanding and encouragement. The individuals I have met in graduate school that I consider friends are too numerous to name. There are a few, however, that cannot go unmentioned. I would specifically like to recognize Abhishek Gumidyala, Manasa Godavarthy Omkar Gurram, Ashwin Badri, Mahesh Sunkula, Joel kodooru, Vamshi Sunchu, Harsha Mandem, Sudarshan Vangala, Vijaykanth Srilam, Jayaram Patibandla, Anish Badri and Jaychandran. Your friendship has made my life at OU more enjoyable and memorable.

I would like to acknowledge the Department of Energy for the research funds, and the chemical engineering department at University of Oklahoma for taking a chance on me. Special thanks to the staff of CBME for their assistance.

Last, but not least, I wish to thank my parents and my sister for their love and support throughout my life. Without them I would have never made it this far in life. They have been there for me every step of the way, have always loved me unconditionally, and supported me during difficult times.

Table of Contents

List of Tables

List of Figures

Abstract

The increasing industrialization and motorization of the world has led to a steep rise in the demand of petroleum-based fuels. However, negative environmental consequences of fossil fuels, natural limitation in their availability and growing concerns over the petroleum supplies has spurred the search for renewable and low carbon emission fuels. Lignocellulosic biomass is one of the most promising renewable and clean energy resources to reduce greenhouse gas emissions and human's dependence on fossil fuels. Moreover, biomass is a continuous energy source and is considered carbon-neutral. Thermochemical conversion of lignocellulosic biomass has received increasing attention as a strategy to produce biofuels from lignocellulosic biomass. Additionally, different thermochemical technologies are being developed/modified so that they can be integrated into the current infrastructure associated with liquid hydrocarbon fuels. Fast pyrolysis of biomass is one of the promising thermochemical technology that produces high yields of bio-oil, but some of the unfavorable properties of bio-oil poses challenges in the development of technical- and cost-effective catalysts and operating processes for the upgrading of bio-oil (1).

In this contribution, we consider thermochemical conversion of oak biomass in multiple stages and understand how the process helps in achieving fractionation of bio-oil and facilitates combating some of the catalytic upgrading problems encountered during bio-oil upgrading. By characterizing the products obtained from each stage, as well as comparing the cumulative carbon yields of the products from stages with fast pyrolysis products carbon yields, further conclusion has been made with respect to the process conditions and potential upgrading strategies for each stage.

Chapter 1: Literature Review

Part of it is extracted from a manuscript in preparation

Christopher Waters, Rajiv Janupala, Richard Mallinson, Lance Lobban

1.1 Introduction

Fossil fuels are the primary energy source for today's electricity generation and transportation fuel supply. Fossil fuels carry several advantages with them such as they are less expensive compared to other sources of energy, simple and cost-effective to transport, generate millions of jobs etc. Along with these advantages, fossil fuels also carry an array of disadvantages with them. Environmental pollution is one of the major consequence of utilization of fossil fuels. Burning of fossil fuels produces carbon dioxide emissions, one of the primary gases responsible for global warming. Besides CO_2, oxides of sulphur and nitrogen are also emitted which eventually cause acid rain. Moreover, fossil fuels are non-renewable sources of energy and their availability is bound to decrease in the future which leads to rise in their prices as well as causes political and economic problems. Therefore, one of the major challenges in the current energy network is to reduce the dependence on fossil fuels and develop a sustainable environmental scenario (4). There is extensive research on different sources of renewable energy as they offer an important alternative in energy consumption as well as diversify the energy sources and contribute to preserving the equilibrium of the ecosystems. In the spectrum of different renewable energy sources such as solar, wind, biomass, water, and geothermal, biomass is the only source that is based on sustainable carbon and this unique advantage of biomass makes it an attractive energy source (5, 6). Lignocellulosic biomass can be available abundantly and may be provide continuous

energy supply. Moreover, biomass is considered a “carbon-neutral” or “zero emission” fuel source because the carbon dioxide released during burning the fuel is again absorbed through the photosynthesis process during biomass growth and forms a part of a carbon cycle (2-4). Therefore, the net accumulation of CO_2 in the atmosphere will decrease by replacing fossil fuels with biomass in the energy supply.

1.2 Structure and Thermal Stability of Biomass Polymers

The main constituents of lignocellulosic biomass are hemicellulose, cellulose and lignin which are linked together to form a composite material. Additionally, biomass also contains water, minor amounts of extractives, and inorganic compounds (ash).

Cellulose is a homopolysaccharide composed of D-glucopyranose units linked to each other by β-(1→4) glycosidic bonds. The main hemicellulose in hardwoods like oak is xylan which is consist of xylospyrano units substituted with acetyl groups at C2 and/or C3 units. Lignin is a crosslinked, heteropolyphenol mainly assembled from three monolignols-sinapyl (S), coniferyl (G), and p-coumaryl (H) alcohols.

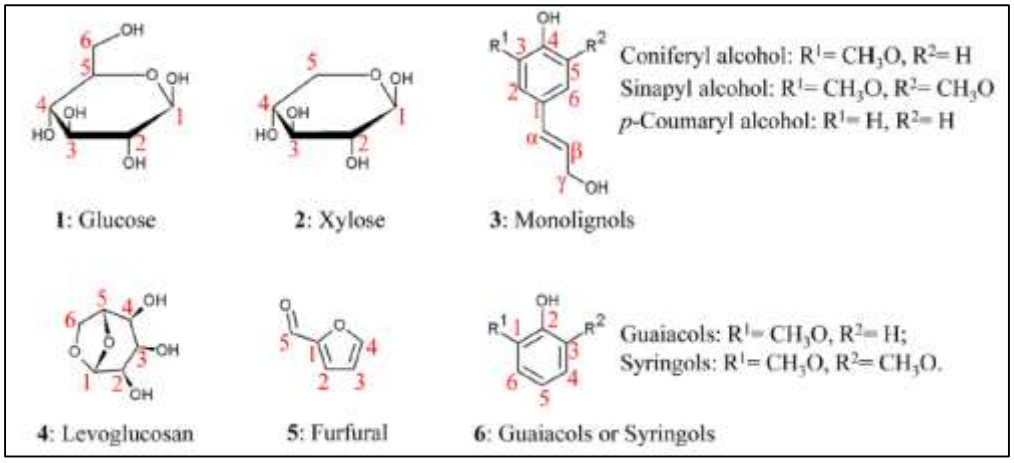

Figure 1.1: Structure of the major basic units of biomass polymers and related products

Each constituent of biomass has a different thermal degradation range which can be used to extract valuable chemicals using a stepwise thermal decomposition process., In general, hemicellulose undergoes thermal degradation in the temperature ranges from 150-350 °C, cellulose is decomposed for the temperatures in the range of 275°C -400 °C, and lignin is featured by broad decomposition for the temperatures between 250 and 500 °C (5, 8).

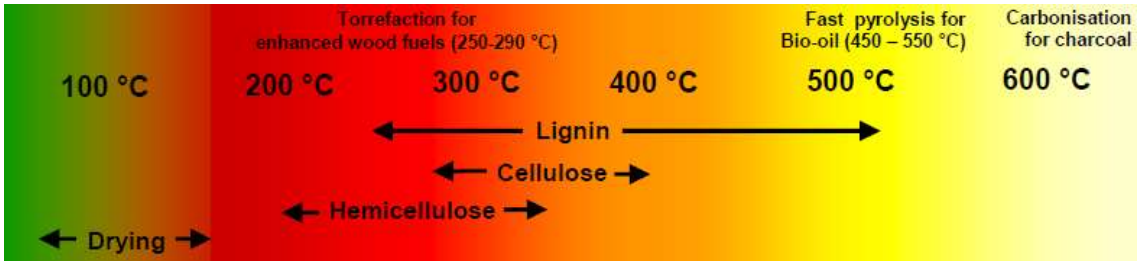

Figure 1.2: Thermal degradation range of biomass polymers (5)

1.3 Thermal Conversion Technologies

Despite the many advantages of biomass as a fuel source, there are some negative properties of biomass such as its high oxygen content, low calorific value (compared to fossil fuels), hydrophilic nature and high moisture content which make raw biomass an expensive fuel to transport and process (7). Because of its hydrophilic nature, biomass storing is a huge problem as the biomass easily absorbs moisture which decreases its calorific value; additional energy and time is needed to dry the biomass before processing. Moreover, improvement in the energy density of biomass is required since a large amount of biomass is needed to replace an equivalent amount of coal in applications such as combustion and gasification (4, 7). As it is also difficult to comminute biomass into small particles, additional processing with associated energy costs is required to reduce biomass into evenly sized small particles. Therefore, the

utilization of lignocellulosic biomass as chemical feedstock faces problems and the challenge is to find a technology that can convert the biomass to fuels and compete with the existing fossil fuels.

Thermochemical conversion of lignocellulosic biomass has received increasing attention as a strategy to produce biofuels from renewable resources (19). The two common biomass thermal treatment processes are pyrolysis and torrefaction. Fast pyrolysis-, is the rapid heating of biomass to 450-600°C with a 1-2 seconds residence time in the absence of oxygen (9-13). Fast pyrolysis converts the solid biomass to a liquid bio-oil with liquid yields as high as 65%, with the remainder of the biomass converted to non-condensable gases (such as CO, CO_2, H_2, CH_4 etc.) and solid carbonaceous char. The primary volatile thermal degradation products are rapidly swept by the carrier gas to escape from the solid residue (char) so that the secondary reactions (which may be catalyzed by the char minerals) are limited.

Torrefaction is another thermal conversion process which is carried out at lower temperatures (250–320°C) for longer periods of time (i.e., residence time in minutes or even hours).[14-19] Torrefaction removes water, CO_2 and light oxygenates and produces a solid residue with a higher energy density and lower O/C ratio than the raw biomass. This improved solid fuel can be used as feedstock for fast pyrolysis and/or gasification.

1.4 Characteristics of Pyrolysis Bio-Oil

The bio-oil produced from the pyrolysis of biomass has some favorable properties similar to that of petroleum fuels, such as low solid content and viscosity. Bio-oils have high carbon content and can be used for the generation of heat and electric power by burning them directly in boilers and gas turbines. They also have low

sulphur and nitrogen content. However the crude bio-oil has several unfavorable properties which limit its utilization as transportation fuel.

Firstly, high oxygen content of the biomass is reflected in the bio-oils which demands for a pre-treatment step to reduce the oxygen content in the feedstock. The oxygen content is around 45-50 wt.% which is much higher than that of petroleum fuels (around 2% in gasoline) Due to the nature of the oxygen moieties, pyrolysis bio-oils are highly reactive. The carboxylic groups such as aldehydes, acids, ketones, ethers react readily to form esters and oligomers during storage. This results in increase in the molecular weight and viscosity of bio-oils due to which phase separation occurs.

Secondly, the pH value of crude bio-oils is around 2.5 due to the organic acids which leads to corrosion of vessels and pipework. Additionally, bio-oils have high moisture content (up to 15-30%), resulting in low heating values. Unlike crude petroleum fuels, distillation of pyrolysis bio-oils produces a solid residue. Bio-oils are not miscible with the hydrocarbon fuels due to the above properties and therefore cannot be integrated into the current petroleum refinery system.

To resolve these issues, catalytic conversion of the bio-oil is required so that it can further be processed in conventional oil refineries. Hydrotreating (removal of oxygen as water by catalytic reaction with hydrogen) of bio-oil is the simplest strategy, but the low H:C ratio of bio-oil leads to very high hydrogen input costs (21). Additionally, hydrotreating of small oxygenates (C_1-C_5 oxygenates), which represent as much as half of the carbon in bio-oil, produces light alkanes (C_2-C_3 alkanes) rather than liquids in the target fuel range (C_6-C_{14}) (1, 21), greatly decreasing the process carbon efficiency.

Another catalytic strategy for whole bio-oil upgrading is the use of zeolite catalysts to convert vapors directly into aromatics (9). While this approach can limit the external hydrogen requirement as compared to hydrotreating, the carbon efficiency of the process is low as the catalysts rapidly deactivate due to high rates of coke formation. Regeneration of zeolites is typically done by combusting away the coke, and the carbon is lost to CO_2. Ultimately, any successful catalytic valorization strategy needs to maximize carbon retention in the product while simultaneously minimizing hydrogen consumption.

1.5 Stage Thermal Fractionation

One strategy that has been proposed to produce simpler intermediate product streams of enhanced purity compared to fast pyrolysis is staged thermal fractionation (also referred to as staged degasification). Staged thermal fractionation leverages the inherent differences in the thermal stability and decomposition products of the biopolymers that constitute biomass. As all three biopolymers yield distinct thermal decomposition products, it should be possible to develop a staged thermal fractionation strategy that is capable of producing several product streams of enhanced compositional purity (Figure 1.3). A low temperature step (stage 1) targeting hemicellulose decomposition is followed by an intermediate temperature step (stage 2) targeting cellulose decomposition, and then a final high temperature step (stage 3) – essentially fast pyrolysis conditions – to decompose the remaining lignin. These purified streams could then be catalytically upgraded using the best catalyst for the job. The thermal segregation comes at the expense of vapor product carbon yield, but the improvement in catalytic performance may offset the carbon yield losses.

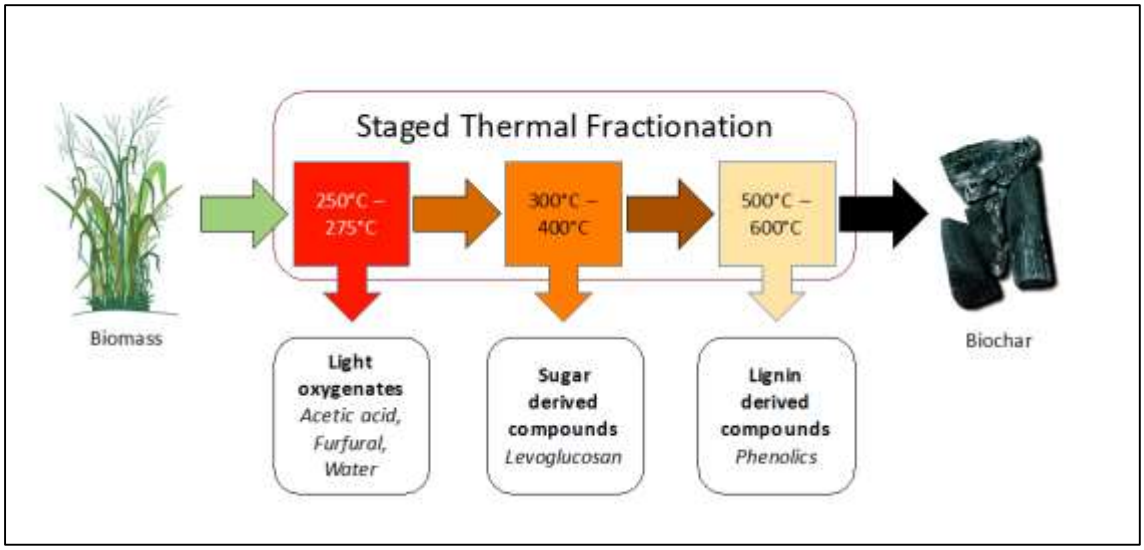

Figure 1.3: Hypothetical configuration of staged thermal fractionation of biomass with resultant product streams from each stage (20)

1.6 Selection of Initial Conditions

With the goal of biopolymer thermal segregation in mind, biopolymer thermal stability regimes in the literature in tandem with a kinetic weight loss model developed specifically for oak biomass by Di Blasi (33) were employed to determine initial experimental conditions (temperature and time) for stage 1 and stage 2 torrefaction.

As previously stated, hemicellulose decomposes at a lower temperature compared to cellulose while lignin decomposes over a broad range of temperatures. Cellulose has been shown to not undergo significant mass loss at temperatures below 275°C (34, 35). As the hemicelluloses are much less thermally stable, a stage 1 temperature not exceeding 275°C should decompose hemicellulose while leaving the cellulose unconverted. Therefore, a temperature of 270°C was selected for stage 1. The residence time for stage 1 is decided by using the kinetic model based on the fact that maximum hemicellulose is decomposed with minimal degradation of cellulose and lignin. Weight loss predictions at different intermediate temperatures (300-400 °C) as a

function of time was plotted to predict the initial conditions for stage 2 keeping in mind that the entire hemicellulose is decomposed, maximum amount of cellulose is degraded and minimal amount of lignin is degraded.

The model results for the conditions selected are presented in table 1.1 and figures 1.4 & 1.5. For the 270°C stage 1, 20 minutes was selected as the process time to achieve conversion of most of the hemicellulose. 360°C for 5 minutes was chosen as the initial stage 2 condition, as the kinetic model predicts near total conversion of the cellulose while most of the lignin is still not thermally degraded. The prediction offered by this kinetic model suggests that the goal of separating the two polysaccharides via thermal degradation is achievable. Additionally, temperatures between 500°C – 550°C has been shown to be an optimal temperature for biomass fast pyrolysis to optimize overall liquid yield (36). Therefore, stage 3 and single step fast pyrolysis was carried out at 520°C.

Temperature/ Time	Predicted cumulative mass conversion	Predicted cumulative Hemicellulose conversion	Predicted cumulative Cellulose conversion	Predicted Cumulative Lignin conversion
270°C, 20 minutes	30.9%	87.3%	2.3%	17.0%
360°C, 5 minutes	61.1%	100.0%	99.0%	18.3%

Table 1.1: Kinetic model weight loss predictions for oak biomass

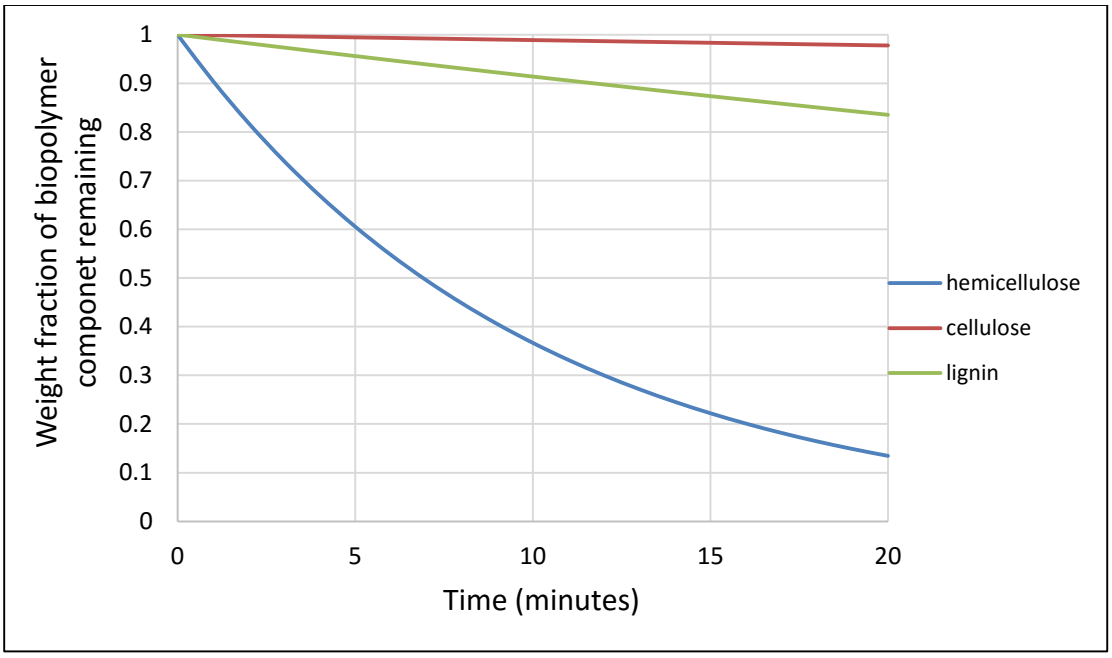

Figure 1.4: Kinetic model weight loss prediction at 270°C

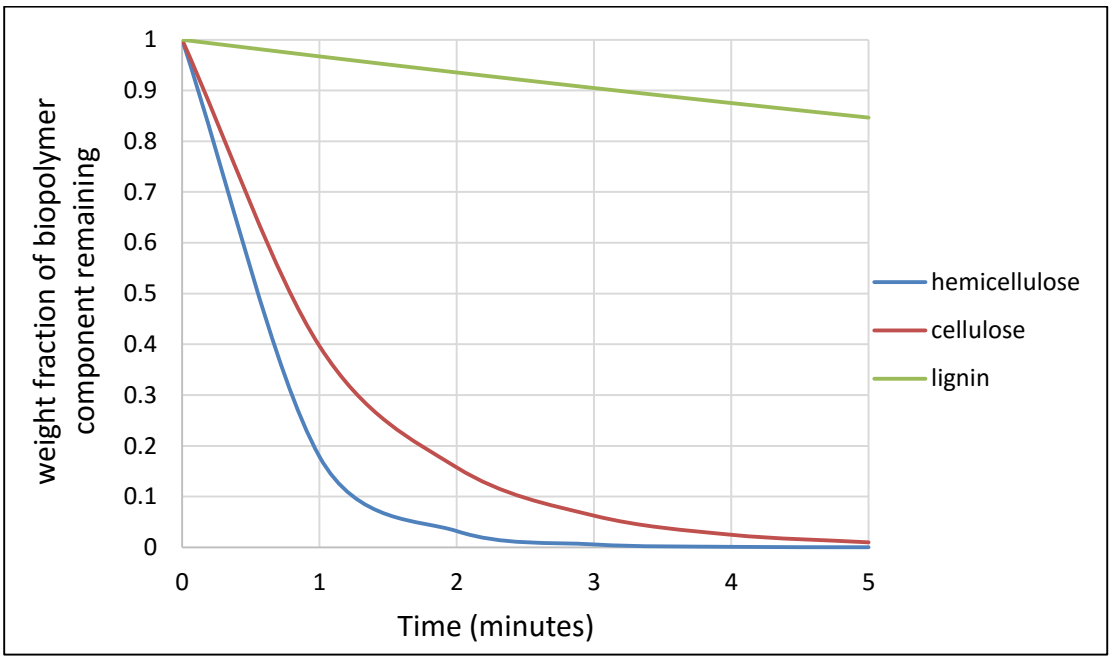

Figure 1.5: Kinetic model weight loss prediction at 360°C

Chapter 2: Experimental

2.1 Feed Material

Red oak sawdust, generated with a table saw from oak boards acquired at a local wood supplier, was used as a starting material for single step fast pyrolysis and stage 1 experiments. Sawdust was sieved to sizes between 425-1000 μm (i.e. sawdust passing through sieve 18 and retained on sieve 40 was collected) before loading into the hopper. For stage 2, the solid product (solid residue) obtained from stage 1 was used as the feedstock, while for stage 3 (or fast pyrolysis), the solid residue produced from stage 2 was the starting material.

2.2 Reactor Description

The bench-scale micro-pyrolysis unit (figure 2.1) consists of a gram scale reactor and utilizes a twin-screw loss-in-weight feeding auger to load the biomass into the reactor. This unit is divided into three sections, viz., feeding section, reaction section and collection section. The entire feeding unit (comprising hopper, twin-screw auger and motor) rests on a 120 kg capacity scale which continuously measures mass of the feeding unit and an automated controls system maintains a constant mass flowrate. A flexible silicone union is used to decouple the reactor from the feeder to minimize the downstream effects on the scale. In the reaction section, a stainless steel reactor with an inner diameter of 22 mm and 0.4 m in length is placed inside an electrical furnace which acts as a heat source and heats the reactor to the desired temperature. The reactor is heated to the desired temperature before the biomass is fed to it. A thermocouple is inserted 8 cm inside the reactor from the bottom to directly measure the biomass temperature. Two streams of nitrogen gas, one to the bottom of the reactor and another

one to the end of the feeding tube (but above the furnace), are used as fluidizing and sweep gas (or carrier gas). Nitrogen gas flowrate for the two streams are monitored and controlled using electronic mass flow controllers (calibration of nitrogen gas flowrate for the two flow controllers is shown in figure A1 in the appendix A). The nitrogen gas with a flow rate of 710 ml/min is pre-heated by flowing through 15 feet of 1/8" stainless steel tubing coiled around the reactor before flowing into the reactor from the bottom.

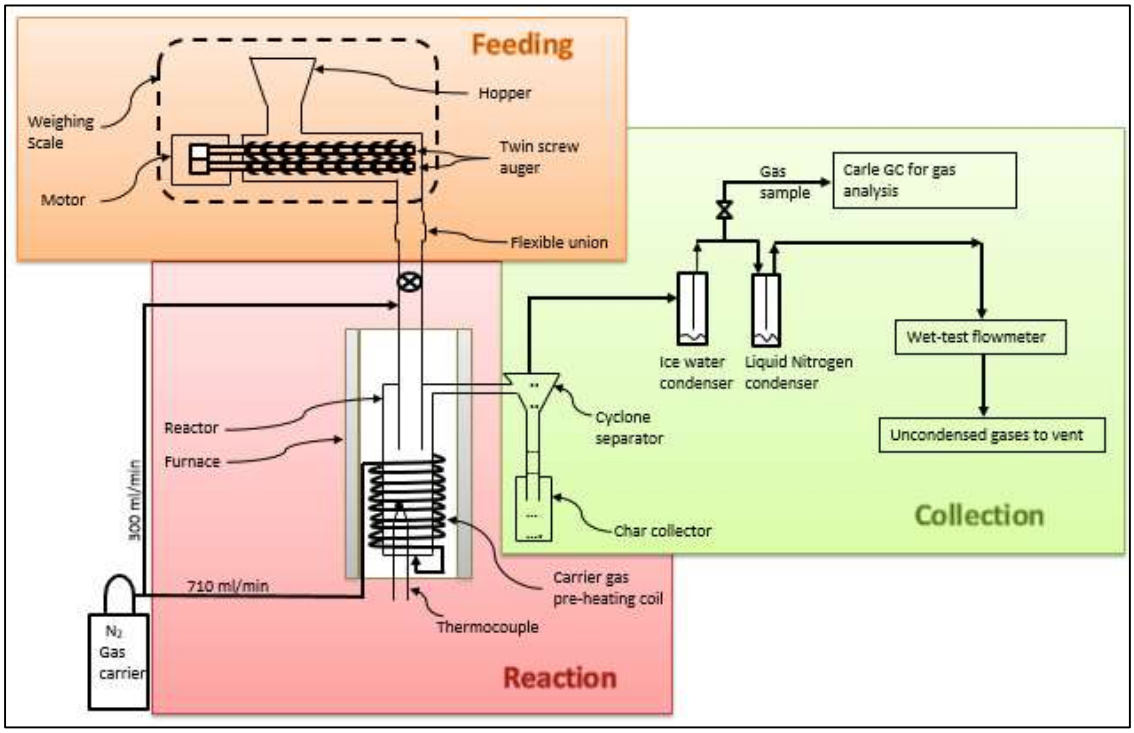

Figure 2.1: Schematic diagram of micro-pyrolysis unit

The pre-heated carrier gas is used both as fluidizing and heat transfer medium, eliminating the need for sand as a heat carrier as in other systems. Additionally, this pre-heated gas sweeps (or carries) the vapors produced inside the reactor to the sequential ice water and liquid nitrogen condensers (or traps) where the vapors are condensed and the liquid is collected for further analyses. The nitrogen flow at the end of feeding tube prevents any vapors produced inside the reactor from entering and

subsequently condensing in the feeding channel. The overall cold nitrogen flowrate from the top of the reactor is low (300 ml/min) to minimize temperature effects inside the reactor. A cyclone separator is positioned in series between the reactor and the condensers to ensure the solid residue is not carried into the condensers along with the effluent gas. The cyclone separator and the tubing between the reactor and the condensers are wrapped with heating tapes and maintained at the same temperature as the reactor to prevent condensation of product vapors. The effluent gas (carrier gas + non-condensable gases) exiting the liquid nitrogen condenser flows through the wet test meter before it is vented. Wet test meter is primarily used to measure the volume of non-condensable gases. Additionally, it can be employed to check for leaks in the system by flowing nitrogen gas at a constant flowrate of 1 L/min (as set by the electronic flow controller) and ensuring it with wet test meter.

2.3 Reactor Limitations

The micro-pyrolysis unit was initially designed and built to operate at steady state pyrolysis conditions (≥450°C) where 80-95% of the biomass was converted to products (liquid + gaseous products); thus large quantities of biomass (20-100 grams) could be fed to the reactor over time before char started accumulating inside the reactor and caused unsteady state conditions. In the case of torrefaction, the conversion to products is not as high as for pyrolysis (29% for stage 1 and 48% for stage 2) and as more biomass is fed, the residue accumulates inside the reactor. The accumulation leads to unsteady state operation and introduces heat and mass transfer effects, unknown secondary reactions, etc. To compensate, the unit is operated as a semi-batch reactor at torrefaction conditions (<450°C) where a batch of not more than 15 grams is rapidly fed

to the reactor. This method of operation limits the ability to collect large amounts of liquid product for the first two stages of torrefaction because of the relatively low liquid product yields. For example, 3.8 g of liquid product is collected at stage 1 conditions (270°C, 20 min.) from a batch of 15.5 g of biomass fed to the reactor, and after various analyses, not enough liquid (<1 g) is left to carry out typical liquid phase catalytic upgrading studies. Hence for each stage, multiple batch runs must be carried out to produce enough liquid product for various analyses and upgrading studies and also generate adequate solid for the subsequent stages.

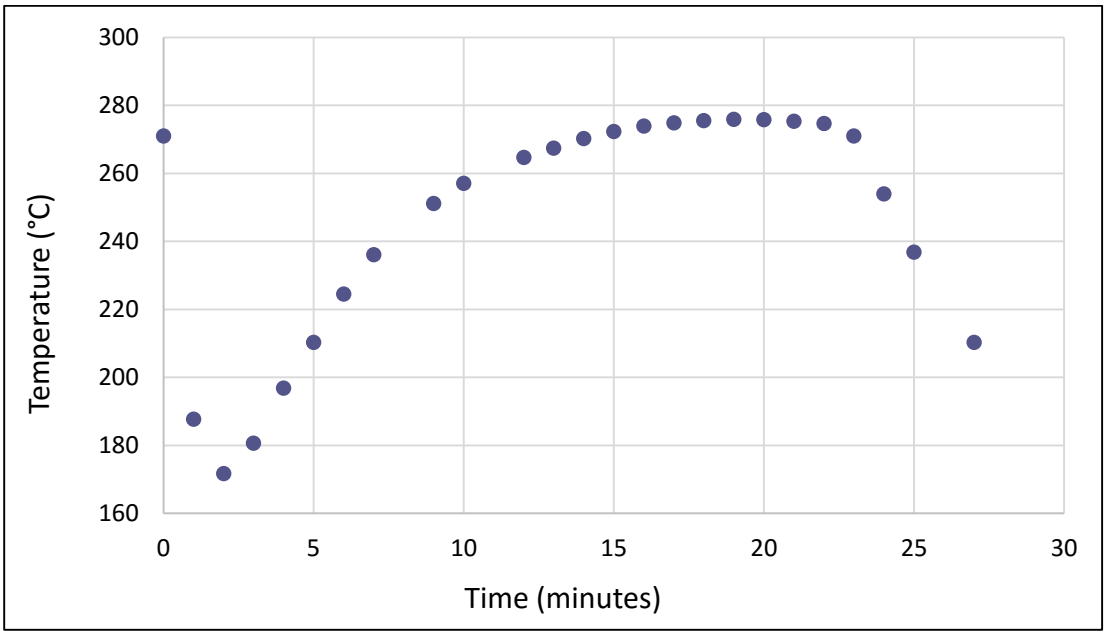

Figure 2.2: Temperature profile of the thermocouple inside the reactor bed at stage 1 conditions

Furthermore, at lower temperatures (<450°C) the reactor operates at unsteady state conditions and, in particular, the biomass temperature changes significantly over the course of reaction time. Figure 2.2 shows the temperature of the thermocouple in contact with the biomass inside the reactor at stage 1 conditions as a function of reaction time. Initially, just before the biomass is introduced into the reactor the

thermocouple placed inside the reactor reads the temperature of carrier gas which is 270°C. As the biomass is fed, the measured temperature decreases to as low as 170°C before increasing to 270°C after 11-12 minutes and further continues to increase slowly beyond 270°C. Even after turning the furnace off at the end of reaction time, the biomass temperature is above 270°C for a few minutes before it starts decreasing. The initial drop in biomass temperature becomes more pronounced as the size of the batch increases. The disadvantage of small batches is low liquid product yield.

2.4 Mass Balance

2.4.1 Feed Quantification

The amount of biomass fed to the reactor is quantified by recording the weight of the feeding unit (resting on top of a 120 kg capacity scale) before and after introducing the biomass into the reactor. This difference in weight of the feeding unit is considered as the mass of biomass fed to the reactor. However, some amount of biomass (generally 0.3-0.5 g) is left behind in the feeding channel (tubing between the outlet of the hopper and inlet of the reactor) and this biomass is quantified by collecting it separately and weighing. Total biomass fed includes the difference in the scale reading minus the biomass left in the feeding channel.

2.4.2 Solid and Liquid Product Characterization

The two glass condensers (or traps) are weighed before and after condensing the vapors and the difference is noted as the mass of the liquid product. The solid product is also recovered and weighed after the reactor has cooled down and analyzed to obtain its elemental composition. Total liquid products include the liquid collected in both the

condensers, while the total solid products include the solid collected in the char collector and the solid inside the reactor.

2.4.3 Non-Condensable Gases Quantification

During the pyrolysis and torrefaction experiments, the non-condensable gases are quantitatively analyzed using a CARLE® Series 400 Analytical Gas Chromatograph (AGC) equipped with a dual thermal conductivity detector. The Series 400 AGC has multi-column/multi-valve capability which enables to quantify C1-C6 hydrocarbons along with CO, CO_2, N_2 and O_2 gases. All the above mentioned gases are selectively adsorbed on different columns and the valves switch position at different times such that the gases are eluted separately and are swept by the helium carrier gas to the TCD detector. Additionally, the Series 400 has a hydrogen transfer system (HTS) incorporated to quantify hydrogen in the gas sample. An internal palladium membrane, at elevated temperature, is selectively permeable to hydrogen. Hydrogen transfers across the membrane into a nitrogen carrier and is detected on a separate TCD. The wide thermal conductivity difference between the nitrogen carrier gas and hydrogen provides linearity and sensitivity impossible to achieve with a helium carrier.

Figure A2 in the appendix shows the calibration curve (TCD area vs Conc. %) of different standard gases. The gas is sampled after the ice water condenser using a 20 ml syringe at different reaction times and injected into the AGC. Effluent gas flowrate is measured using wet test meter after each gas sample. Condensation of carbon dioxide (the major non-condensable gas) in the liquid nitrogen condenser mandates sampling the gas between the two condensers. PeakSimple Chromatography Software from SRI Instruments is used to integrate the peaks and get the TCD area. After obtaining the

peak area, the calibration curves are used to estimate the concentration (mole %) of non-condensable gases in the injected samples. Finally, the amount of non-condensable gases in terms of grams is calculated by using the effluent gas flowrate and assuming STP conditions (one mole of an ideal gas at STP occupies 22.4 liters). The instrument is checked for its repeatability once a month or whenever questionable behavior is observed by recalibrating it with a standard gas mixture.

One of the assumptions in quantifying the amount of non-condensable gases is approximating the effluent gas flowrate to carrier gas flowrate since some of the non-condensable gases are condensed in the liquid nitrogen condenser. However, these gases are evaporated once the condenser is removed out of the liquid nitrogen bath. Additionally, the amount of C3-C6 hydrocarbons is assumed to be negligible. The Carle AGC has two sample inlet ports; Sample Inlet I & Sample Inlet II. In order to measure C1-C6 hydrocarbons along with CO, CO_2 and H_2, the gas sample must be injected through inlet II but the method is 40 minutes long. Therefore, injecting multiple gas samples collected during a single experimental run is not possible as there is a probability for the gases to escape from syringe. For the gas sample injected through inlet I, the method is 12 minutes long but only CO, CO_2, H_2, CH_4, C_2H_6 and C_2H_4 gases can be quantified. Thus, multiple gas samples can be analyzed with this shorter method but at the cost of assuming the amount of C3-C6 hydrocarbons is insignificant.

2.5 Characterization Techniques for Solid and Liquid Products

The condensed liquid in both the traps is recovered into the same glass vial using a pipette and then analyzed using various techniques to obtain a detailed product

distribution and elemental composition. The solid product is also analyzed to get its elemental composition.

2.5.1 Water Quantification

The water content (wt.%) in the condensed liquid products is quantified using METTLER-TOLEDO V20 Volumetric Karl Fischer Titration Unit, which is capable of measuring water contents in the range of few 100 ppm to 100%. Figure 2.3 shows the setup of the Karl Fisher Unit. HYDRANAL®-Composite 5 titrant and HYDRANAL®-Solver (crude) oil solvent are the two conventional reagents used to determine the water content in bio-oils. Typically, 0.01-0.1mg (depending on the water content in the liquid sample; larger amount in case of lower water content) of liquid sample is injected into the titration cell using a syringe and the result is displayed as weight percent (wt. %) of the injected amount. Multiple injections are carried out to check for repeatability and the average is considered as amount of water present in the entire liquid product. The titrant is often (preferably every day) standardized by using HYDRANAL®-Water Standard 10.0 (water content = 1 wt. %) to examine for any contamination (probably by absorption of air humidity by the titrating reagent). In case of any contamination (which can be concluded based on the measurement of water % for water standard 10.0), the titrating reagent is replaced.

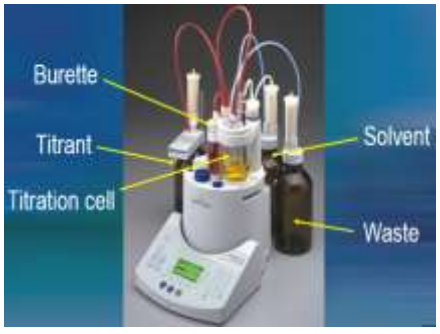

Figure 2.3: Mettler-Toledo V20 Karl-Fischer Volumetric Titration Unit

2.5.2 Elemental Composition

The carbon, hydrogen, and nitrogen content in the liquid and solid products as well as of the raw biomass (raw oak) is measured using a CE-440 Elemental Analyzer, purchased from Exeter Analytical, Inc. Oxygen content is obtained by difference based on the assumption that the amount of other elements (S, Mg, Ca, K, N, etc.) in biomass and solid and liquid products is negligible. Due to its chemically inert nature and high thermal conductivity, helium gas is used to carry the combustion products through the analytical system to atmosphere, as well as for purging the instrument. The weighed sample is introduced into a high temperature furnace and passes through combustion and reduction chambers to finally produce CO_2, H_2O and N_2 gases. The sample gases are then carried into a mixing volume chamber where they are homogenized at precise volume, pressure and temperature. Finally, the homogenized mixture passes through three pairs of thermal conductivity cells with adsorption traps between each pair of cells selectively adsorbing water in the first trap and carbon dioxide in the next trap. The differential signal read before and after each trap reflects the concentration of water and carbon dioxide and, therefore, the amount of hydrogen and carbon respectively in the original sample. The nitrogen concentration is measured by comparing the output signal of the remaining gas (gas after second trap, i.e. nitrogen and helium) obtained from the final thermal conductivity cell to the one obtained from a reference cell though which pure helium flows.

Typically, the mass of the solid and liquid samples introduced into the analyzer are 1-3 mg and 1-5 mg, respectively. It is observed that the CE-440 shows greater error in measuring C/H/N for liquid samples compared to solid samples due to sample

evaporation, especially with highly volatile liquid samples. The error can be reduced by minimizing the time between sample preparation and its introduction into the analyzer.

2.5.3 Organic Compounds Identification and Quantification

Capillary Gas Chromatography (GC) is the most powerful technique for the separation of pyrolysis products, while mass spectrometry (MS) and flame ionization detection (FID) are the most suitable methods for compound identification and quantification, respectively, in association with the GC technique.

A known amount of liquid product is diluted in known amount of solvent (usually ethanol) and 1µl of this liquid mixture is injected into a Shimadzu QP-2010S GC/MS-FID system via a Shimadzu Auto Injector AOC20i. A 60m long semi-polar RTX-1701 column (25µm diameter, 0.025µm film thickness) is used with the temperature program on the column beginning at 45°C for 2 minutes, then increasing at a rate of 3°C/min for 78.33 minutes to a final temperature of 280°C, held for 20 minutes. The mass spectrometer scanned masses from m/z 35.00 to 250.00 at 0.5 seconds per scan. The resulting ion chromatogram was used to identify significant peaks in the chromatogram.

Two publications by Faix et al. (22, 23) were used as the primary means of compound identification. As Faix et al. used a 15m DB-1701 column, the retention order (but not absolute time) of the pyrolysis products they observed are the same as in this work, and additionally they list the base peak (intensity 100%) mass along with intensities of nine other abundant masses which eases the compound identification. In the case that a peak was unable to be identified using these two publications, the peaks were either assigned identifications based on NIST library search, assigned to

compound lumps based on major ions, or left unidentified. Identified compounds were assigned into lumps of compounds (or compound groups) based on organic functionalities, in a similar manner to that described by Dauenhauer et al. (24).

The identified peaks from the ion (or MS) chromatogram were then matched to the corresponding peaks from the FID chromatogram. The area of each of the peaks were then determined by integration. Calibration of the FID was performed by injecting varying concentrations of phenol in methanol at known quantities to develop a response curve (calibration curve for phenol is shown in figure A3 in the appendix). For each identified compound in the liquid product, the response factors (grams/area) were calculated using the effective carbon number (ECN) model in tandem with the phenol calibration curve. Table 1 in the appendix lists the response factor, effective carbon number and compound group of all the compounds identified in this study. Based on the area of each compound obtained from integration, their respective response factors from ECN model and the dilution ratio of liquid product to the solvent injected into the GC, the mass of each compound in the liquid product is calculated and finally the carbon content of the liquid product is computed.

2.6 Carbon Balance

After obtaining a detailed compound distribution of liquid product and non-condensable gases along with elemental composition of feed and solid product, carbon balance for each experiment is computed. While the amount of carbon in the feed and solid product is obtained from elemental analysis, the carbon content in the liquid product can be obtained either from elemental analysis or from GC/MS-FID analysis. Also, the carbon in non-condensable gases is computed from Carle GC.

2.7 Oligomers Quantification

Even though the liquid product is analyzed soon after it is produced to minimize the secondary reactions during storage, there is still a possibility for the formation of oligomers especially at higher reaction temperatures due to presence of different functionalities in the liquid product. Therefore, it is important to quantify these oligomers and study their impact during liquid phase catalytic upgrading. Unfortunately, these compounds are present in the invisible portion of GC chromatogram i.e. they cannot be detected by GC/MS-FID. However, these compounds can still be combusted at high temperatures and thus the carbon content of the liquid product obtained from elemental analyzer also includes that of oligomers as well. Therefore, the difference in the carbon content of the liquid product measured from elemental analysis and GC/MS-FID analysis is assigned to oligomers.

Chapter 3: Stage 1 Torrefaction

The stage 1 thermal treatment or stage 1 torrefaction or low temperature torrefaction is operated at nominal conditions of 270°C for 20 minutes. A known amount of raw oak (not oven dry) is loaded into the hopper and the reactor is pre-heated to 270°C. The oak is fed to the micro-pyrolysis reactor using the twin screw feeder at a nominal rate of 15 g/min. The amount of oak left over in the hopper is recovered after the reaction and weighed to get the amount of oak fed to the reactor and also confirm it with the feeder scale reading. A batch of typically 15.5 g of oak is introduced into the reactor within a short time (here in one minute) so that all the oak particles are inside the reactor almost for the same time (maximum variance in residence time of solid is one minute).

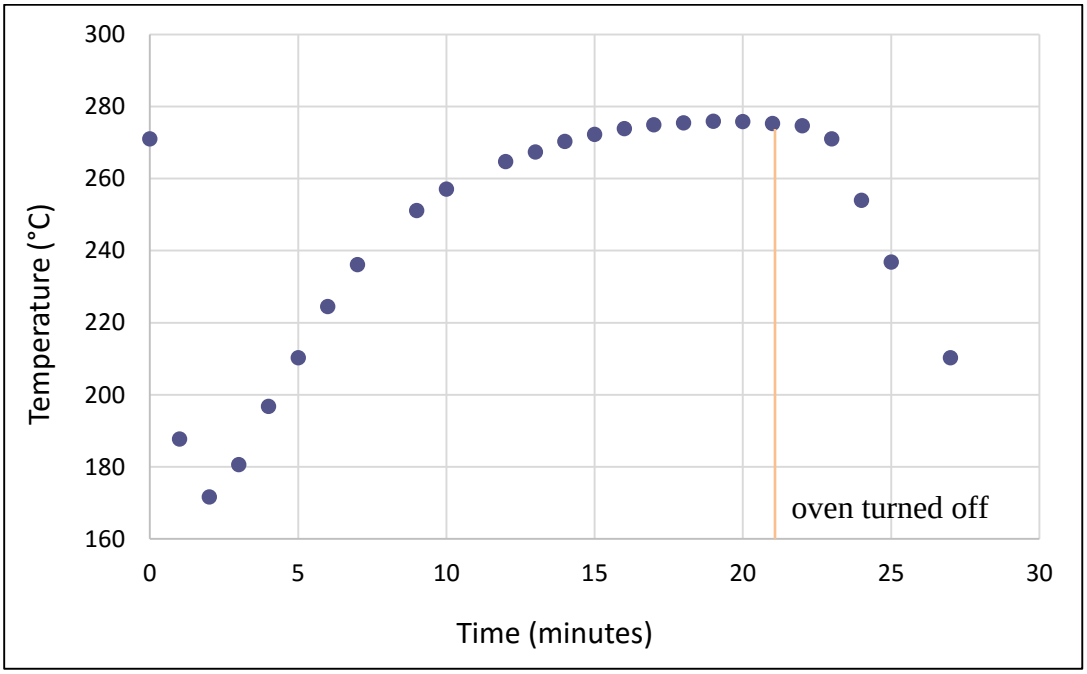

Figure 3.1: Temperature profile of thermocouple inside the reactor at stage 1 conditions

Figure 3.1 depicts the changes in temperature of oak measured using the thermocouple in the oak bed from the moment the oak feeding starts until its temperature falls below 200°C after the oven is turned off. At t = 0 minutes, the temperature measured is that of pre-heated carrier gas. Due to limitations in the reactor design as described in the experimental section, oak is not maintained at 270°C for the entire 20 minutes. Once the oak is introduced into the reactor, the thermocouple reading falls to as low as 170°C and then a dynamic heating period is observed for about 12 minutes till the thermocouple reads 265°C. The temperature measured here is the temperature of the thermocouple that is at the center inside the reactor. The oak particles that are in contact with the thermocouple show similar reading as that of the thermocouple but a temperature gradient exists from center to walls of the reactor. After the dynamic heating period, changes in the thermocouple readings are small and it reads temperatures between 265°C and 275°C for 11 minutes. The vapors are collected until the temperature of oak falls below 200°C when it is assumed that further decomposition of biomass is negligible.

3.1 Mass Balance

Mass balance for the entire stage 1 batch run is obtained by noting down the difference in feeder scale reading for the amount of oak fed to the reactor, weighing the solid residue inside the reactor, quantifying the non-condensable gases with Carle-GC and weighing the liquid condensed in the traps.

Carbon dioxide and carbon monoxide are the only two non-condensable gases observed at low temperature torrefaction and are quantified by Carle AGC equipped with TCD detector. A plot of GC area vs. the time at which different gas samples were

taken is shown in Figure 3.2 and the total area under the curve is calculated by assuming straight lines between two successive points. Finally, the amount of non-condensable gases is computed using calibration curves for CO and CO_2, measuring effluent gas flowrate with wet-test meter and assuming standard conditions.

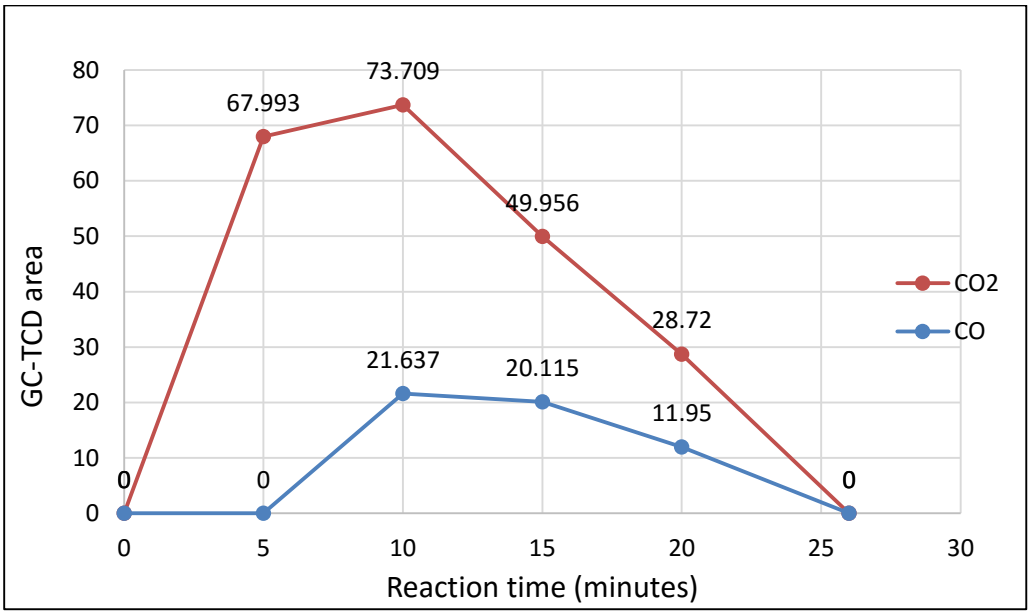

Figure 3.2: GC-TCD area of non-condensable gases sampled at different reaction times during stage 1 torrefaction and injected into Carle-GC

Table 3.1 shows the overall mass balance for stage 1 torrefaction. The overall yield of products accounts to 99% and the remaining unaccounted mass (1%) can be attributed to a combination of different things. Primarily, some of the vapors may not be condensing in the traps which would lead to lower mass balance. Another significant source of uncertainty is that, the present technique of measuring the biomass fed to the reactor is accurate to 0.2g. This results in random errors where the amount of biomass fed to the reactor could sometimes be lower or higher or same as what the difference in the feeder scale reading shows. Finally, some of the minor reasons that contribute to the un-weighed mass could be inaccuracy of the balance used for weighing the products

and assumption of straight lines between successive points in the quantification of non-condensable gases.

Oak fed to the reactor	15.5 gm	100%
Stage 1 solid residue	10.8 gm	69.7%
Stage 1 liquid product	3.9 gm	25.2%
Non-condensable gases	0.63 gm	4.1%
Unaccounted mass	0.17 gm	1.0%

Table 3.1: Mass balance for stage 1 thermal treatment

3.2 Liquid Product Characterization

Major compounds identified in stage 1 liquid product are water and organic compounds such as acetic acid, furfural, acetol, light oxygenates and lignin-derived methoxy phenols. The water content was determined by Karl-Fischer titration to be 50.3% by weight. Organic compounds are quantified by FID analysis. Nearly 86% of the total FID area is identified and assigned to different organic compounds and the remaining unidentified area is evenly distributed to all the identified peaks. The mass of each compound in the liquid product is calculated by using their respective response factors obtained from ECN model in combination with phenol response curve. A detailed sample calculation to obtain the mass of acetic acid present in the liquid is provided in Appendix B. Similarly, the amount of all the other identified organic compounds present in the liquid are also computed. After most of compounds present in the liquid product are identified and quantified, they are lumped into groups.

Figure 3.3 shows the selectivity of different compounds lumps present in the liquid collected from stage 1 thermal treatment. Water and acetic acid constitute 73% of

the total liquid mass. The relatively low selectivity to phenolic species and anhydrous sugars confirm that at these mild conditions, hemicellulose breakdown is the primary source of the volatile products formed. About 94% of the total liquid product is accounted by water and organic compounds and the remaining 6% which is not measured is indicated as "undetected" in figure 3.3. There are several things that contribute to this unquantified mass either by FID analysis or Karl-Fischer titration. Firstly, acetic acid and furfural existing in the stage 1 liquid can engage in different reactions and form high molecular weight oligomers which cannot be detected by the GC column. Secondly, the response factors predicted from ECN model could be different from the one obtained by manual injections. Another minor reason could be the inaccuracy of the Karl-Fischer titration unit in the measurement of water content.

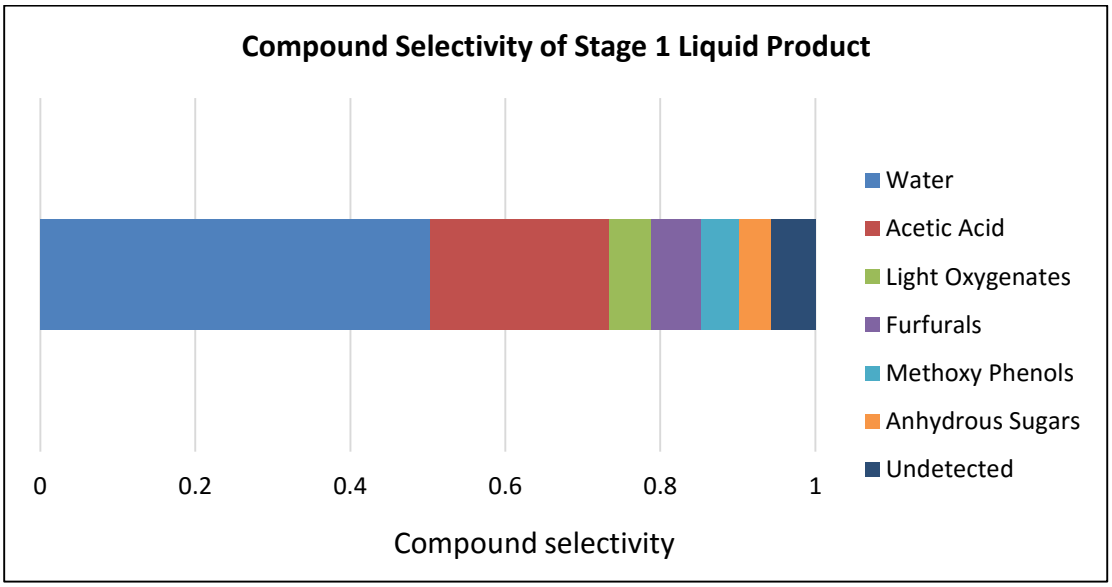

Figure 3.3: Gram selectivity of compounds present in stage 1 liquid product separated by compound groups

The carbon content measured in the condensed liquid product from stage 1 with respect to oak is shown in figure 3.4 and sums to 51.38 mg of carbon/gram of oak.

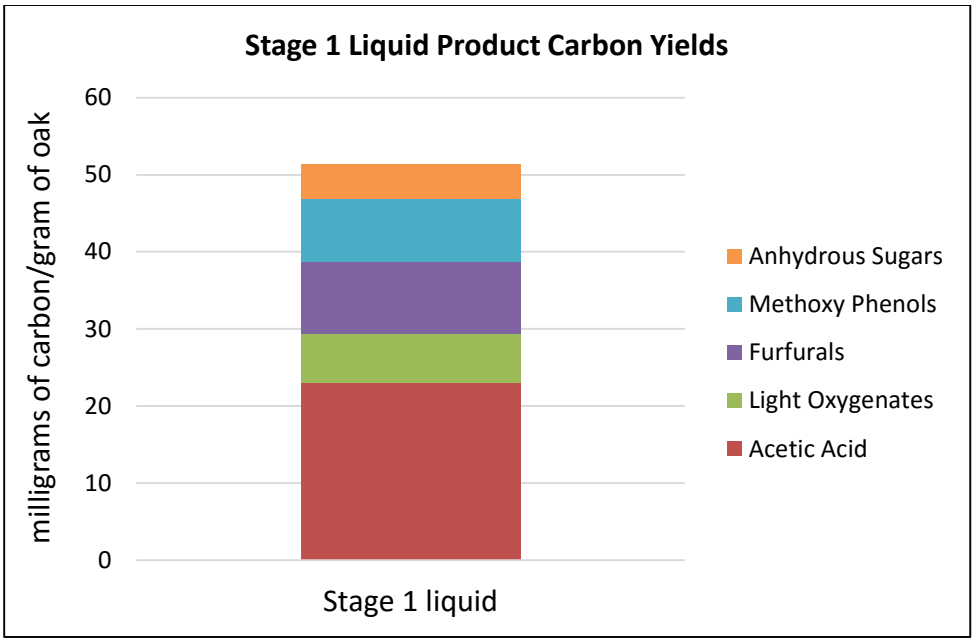

Figure 3.4: Stage 1 liquid carbon yields separated by compound groups

3.3 Carbon Balance

Carbon and hydrogen content in solid and liquid products as well as in the raw biomass is measured using elemental analyzer while the oxygen content is taken as the difference assuming the amount of nitrogen, sulphur and other minerals is negligible.

Sample	% C	% H	% O
Oak	46.21	5.88	47.91
Stage 1 liquid product	25.82	8.33	65.85
Stage 1 solid residue	51.94	53.67	42.39

Table 3.2: Carbon, hydrogen and oxygen content in oak and solid and liquid products from stage 1 thermal treatment as measured with elemental analyzer

	grams of carbon	Yield
Oak fed to the reactor	7.16	100%
Stage 1 solid product	5.61	78.4%
Stage 1 liquid product	1.01	14.1%
Non-condensable gases	0.19	2.6%
Balance	0.35	4.9

Table 3.3: Carbon balance of stage 1 thermal treatment

Table 3.3 shows the overall carbon balance for stage 1 torrefaction. The grams of carbon present in different materials are calculated based on their masses as provided in Table 3.1 and their respective carbon weight percentage as given in Table 3.2. About 5% of the carbon in oak is not recovered in any of the products and this could be due to carbon lost in the unrecovered mass as reasoned in mass balance section. Moreover, some mass of the liquid condensed in the traps is not recovered into glass vial (mainly because it is condensed on the walls of the traps) (but its mass is taken into consideration in mass balance) and it is assumed that the composition of this unrecovered liquid is the same as the recovered one. However, the FID chromatogram (Figure 3.4) of the unrecovered liquid shows that it is more concentrated in higher molecular weight compounds. Therefore, the carbon content of the liquid product will likely be higher than calculated assuming the same composition in the unrecovered liquid. Nevertheless, the unrecovered liquid mass only constitutes 10-15% of the total liquid product so the increase in carbon content will be small. The liquid sticking on the walls of the condensers is recovered by diluting in solvent but diluting complicates the

quantification of carbon content by elemental analysis and FID analysis due to evaporation of solvent.

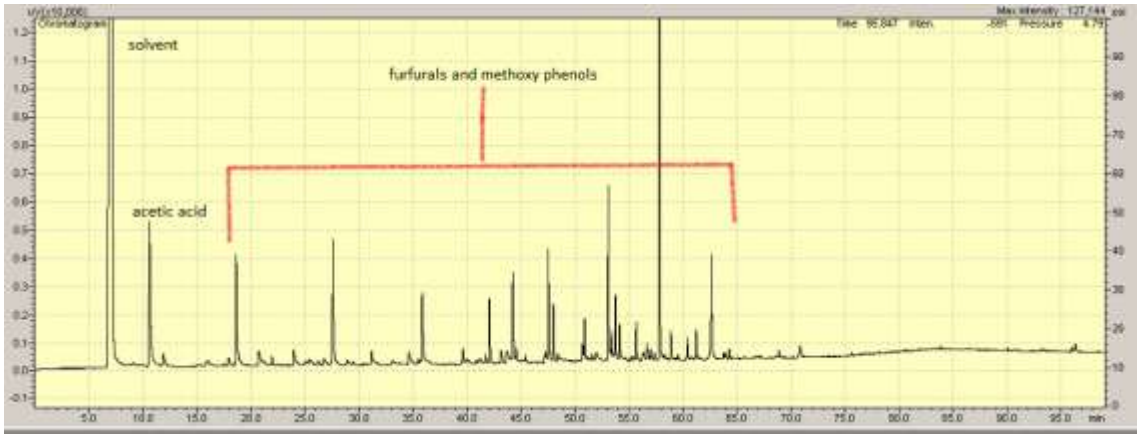

Figure 3.4: FID chromatogram of the stage 1 liquid remaining in the liquid nitrogen trap diluted with methanol

The carbon content of the liquid product can be quantified either by elemental analysis or by FID analysis. Figure 3.5 shows the carbon yield of stage 1 products with the only difference between the two columns being the carbon content in the liquid product as quantified with different analyses. The carbon content in stage 1 liquid product measured from elemental analysis is 20% more than that obtained from FID analysis. The major reason for the difference in carbon content as quantified by these two analyses could be due to the presence of oligomers. While the carbon in oligomers could still be combusted and measured by the elemental analyzer, this carbon passes through the GC undetected and is eventually not quantified by the FID. Additionally, in the case of FID analysis, the unidentified area (about 14% for stage 1) is evenly distributed among all the compounds. These unidentified compounds are mainly present in latter part of the chromatogram (after 20 minutes retention time) where furfurals and methoxy phenols are evolved and they have higher carbon to oxygen ratio (>2:1)

compared to the light oxygenates (carbon to oxygen ratio is ≤ 1 for most of the compounds) observed at lower retention times.

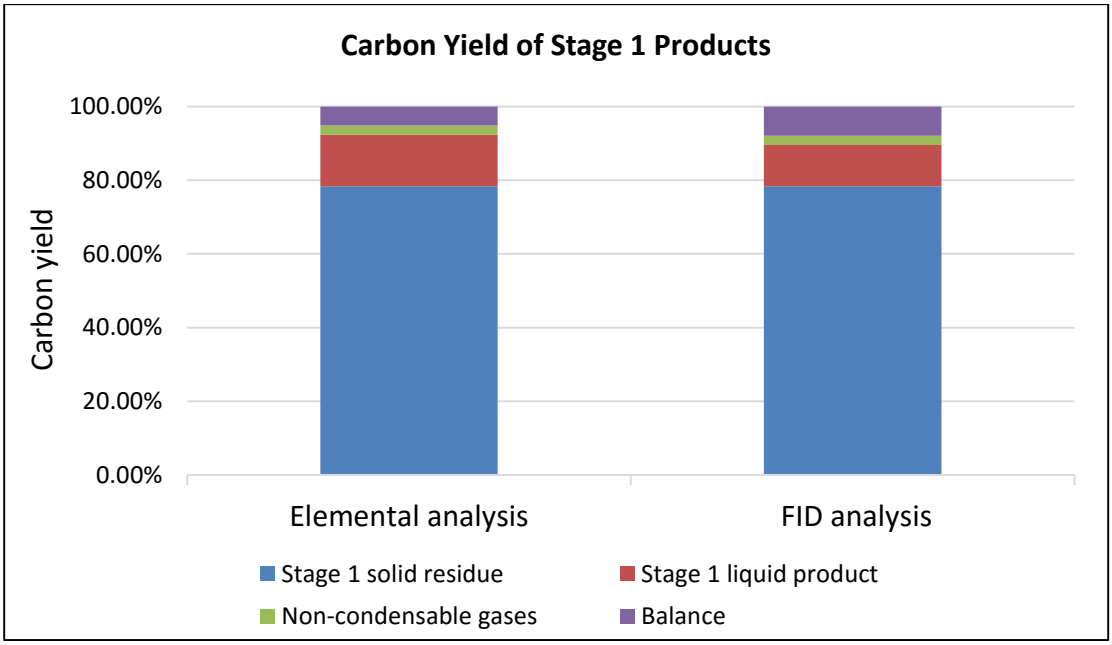

Figure 3.5: Carbon yield of different stage 1 products with carbon in stage 1 liquid product quantified by both elemental analysis and FID analysis

Chapter 4: Stage 2 Torrefaction

The stage 2 thermal treatment or stage 2 torrefaction or intermediate temperature torrefaction is operated at nominal conditions of 360°C for 5 minutes. The solid residue obtained from stage 1 thermal treatment is the starting material. Typically, for stage 2 torrefaction, a batch of approximately 10 g of stage 1 residue (which can be obtained from a single stage 1 batch run of about 15 g) is fed into the reactor. However, several batches of stage 1 torrefaction are carried out to collect enough stage 1 solid for several stage 2 batch experiments. The maximum difference in the carbon content in stage 1 solid obtained from different stage 1 runs is less than 5%, so the solid obtained from different stage 1 batch runs is mixed. Similar to stage 1 thermal treatment, the feed is introduced into the reactor at a nominal rate of 15 g/min within 40 seconds so that the residence time of all particles inside the reactor is almost the same.

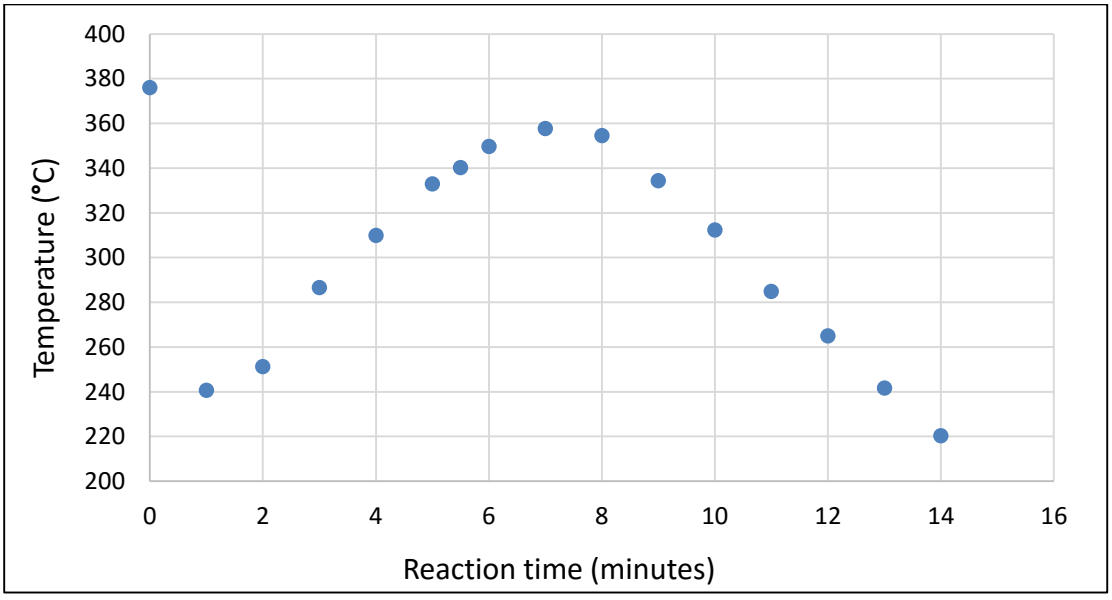

Figure 4.1: Temperature profile of thermocouple inside the reactor at stage 2 conditions

Figure 4.1 shows the changes in thermocouple reading during stage 2 thermal treatment where we notice a similar decrease in thermocouple temperature as that of the stage 1 once the biomass is introduced into the reactor followed by a temperature increase when the feeding is complete. The thermocouple measures the temperature of the biomass around it and there exists a temperature gradient from the center to the walls of the reactor. The vapors are collected until the temperature of stage 1 residue falls below 220°C. It is assumed that no further decomposition of biomass occurs.

4.1 Mass Balance

Similar to stage 1 torrefaction, multiple gas samples are taken during reaction and injected into the Carle-GC to quantify the non-condensable gases in stage 2 vapors. CO_2 and CO are the major compounds identified and a small peak of methane is observed but not big enough to get an integration area.

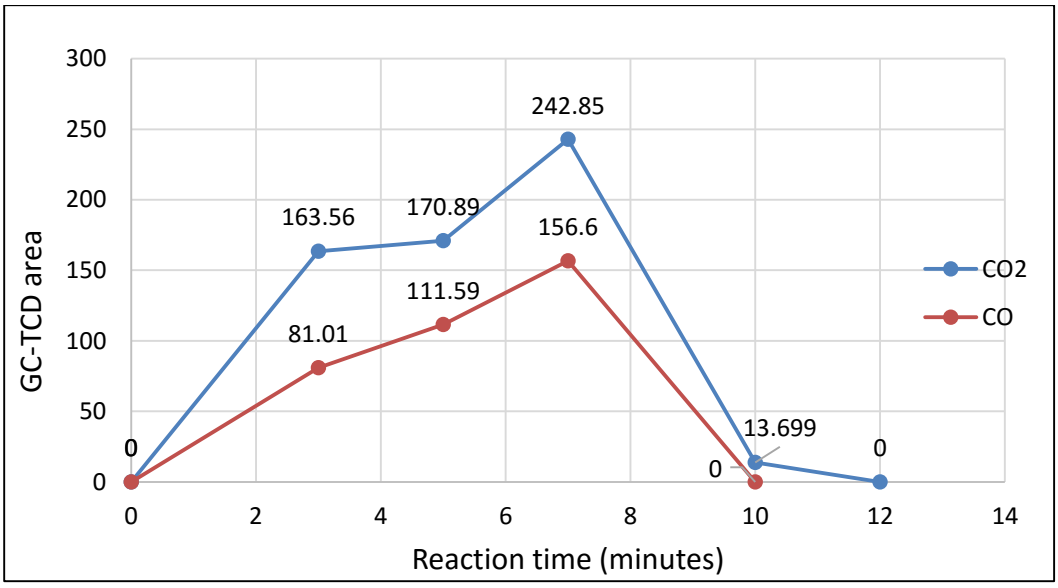

Figure 4.2: GC-TCD area of non-condensable gases sampled at different reaction times during stage 2 thermal treatment

Table 4.1 shows the overall mass balance for a single stage 2 torrefaction batch experiment. About 95% of the stage 1 residue is recovered in the products.

Stage 1 solid residue (feed)	9.7 gm	100%
Stage 2 solid residue	4.4 gm	45.4%
Stage 2 liquid product	4.0 gm	41.2%
Non-condensable gases	0.80 gm	8.2%
Unaccounted mass	0.50 gm	5.2%

Table 4.1: Mass balance for stage 2 thermal treatment

4.2 Liquid Product Characterization

During stage 2 thermal treatment, any remaining hemicellulose is expected to decompose along with significant cellulose and lignin decomposition. As a result of cellulose decomposition, a significant fraction of sugar derived compounds is expected in the stage 2 liquid product. Levoglucosan is a major cellulose decomposition product and to lesser extent furanics which are also a sugar derived class of molecules should be observed. The water content was determined by Karl-Fischer titration to be 33.5% by weight. A know concentration of stage 2 liquid and ethanol (solvent) is injected into the GC/MS-FID.

Figure 4.3 shows the selectivity of different compounds lumps present in the liquid collected from stage 2 thermal treatment. Levoglucosan constitutes 16.2% of the total liquid product and is the largest single organic compound present in the liquid stream. As cellulose pyrolysis is not a major producer of acetic acid (26), any acetic acid formed in stages 2 and 3 must come from decomposition of any remaining unreacted hemicellulose and from lignin decomposition (25). The high selectivity of water in

liquid product also points towards incomplete decomposition of hemicellulose (although water as a reaction product is also likely from cellulose and lignin decomposition). Having knowledge about the content of biopolymers in the torrefied solid could facilitate prediction of optimum residence time at different temperatures for stage 1.

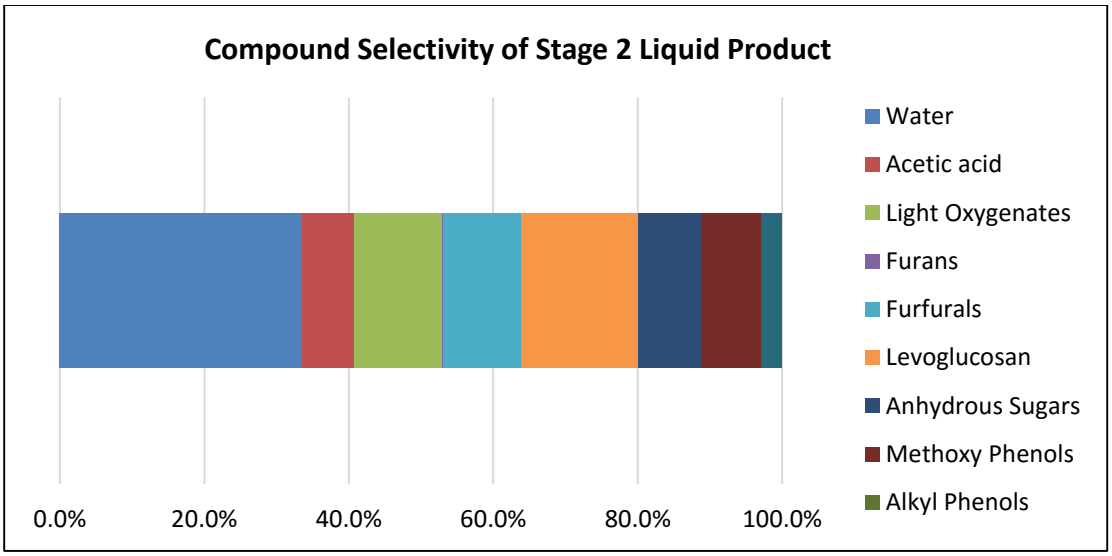

Figure 4.3: Mass selectivity of compounds present in stage 2 liquid product separated by compound groups

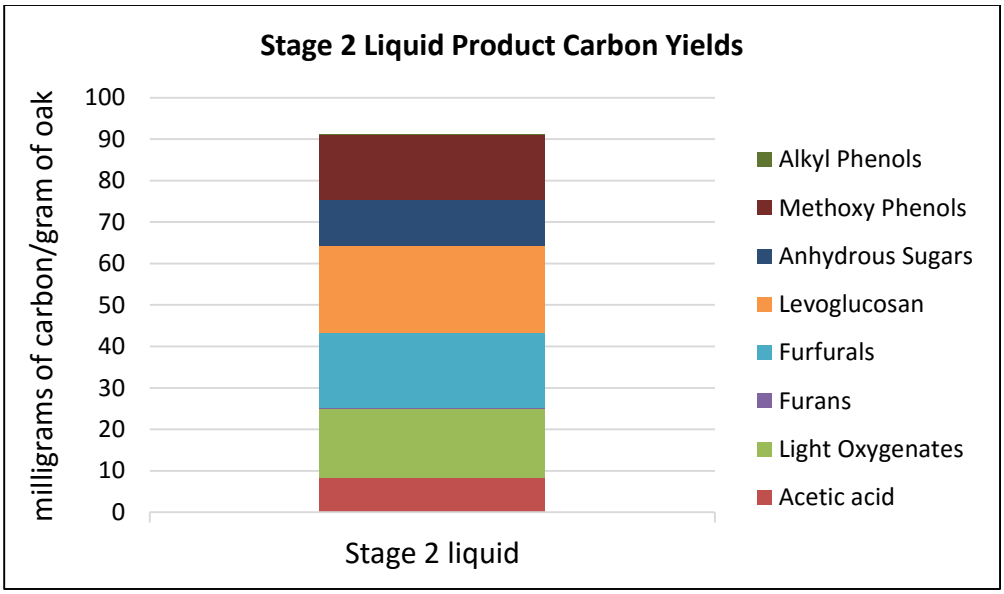

Figure 4.4: Stage 2 liquid carbon yields separated by compound groups with reference to raw oak

The carbon content measured in the condensed liquid product from stage 2 with respect to oak is shown in figure 4.4 and sums to 91.1 mg of carbon/gram of oak

4.3 Carbon Balance

Sample	% C	% H	% O
Stage 1 solid residue (feed)	51.96	5.75	42.28
Stage 2 liquid product	35.03	7.56	57.41
Stage 2 solid residue	67.65	4.91	27.44

Table 4.2: Carbon, hydrogen and oxygen content of feed and solid and liquid products as measured by elemental analyzer for stage 2 thermal treatment

Table 4.3 show shows the overall carbon balance for stage 2 torrefaction. The grams of carbon present in different materials are calculated based on their masses as provided in Table 4.1 and their respective carbon weight percent as given in Table 4.2. About 92% of the carbon present in stage 1 residue is accounted for in the products.

	grams of carbon	Yield
Stage 1 residue fed to the reactor	5.04	100%
Stage 2 solid product	2.94	59%
Stage 2 liquid product	1.44	27.8%
Non-condensable gases	0.24	5.1%
Unaccounted carbon	0.42	8.1%

Table 4.3: Carbon balance for stage 2 thermal treatment

About 8.1% of the carbon in stage 1 residue is not accounted for in the products and this could be due to combination of many reasons like loss of carbon in the unaccounted mass, evenly distributing the carbon present in unidentified peaks (mainly phenolics and furfurals) to all the compounds and assuming the composition of the unrecovered liquid in the traps is the same as the recovered liquid when it is concentrated in longer carbon chain molecules.

Chapter 5: Stage 3 Torrefaction & Single Step Fast Pyrolysis of Oak

The stage 3 thermal treatment or stage 3 torrefaction and single stage fast pyrolysis of oak are both carried out at similar conditions of 520°C with the residence time of the vapors inside the reactor less than 5 seconds. Unlike stages 1 & 2, the biomass is introduced into the reactor at low nominal rate of 1 g/min because the biomass undergoes decomposition as soon as it is introduced into the reactor and little or no further decomposition happens as the biomass resides inside the reactor. Due to the introduction of biomass at a low rate, the temperature profile of the thermocouple inside the reactor is almost a straight line with the maximum observed drop in temperature of ~5°C. While stage 2 solid residue obtained from stage 2 thermal treatment is the starting material for stage 3 torrefaction, raw oak is the starting material for single step fast pyrolysis. Fast pyrolysis of oak is considered as a base case for comparison purposes – i.e., the cumulative product yields/carbon yields obtained from three stage thermal treatment is compared with product yields/carbon yields from single step fast pyrolysis However, it must be emphasized that the purpose of the three stage treatment is not increased total yield, but rather decreased complexity of the intermediate streams to facilitate subsequent upgrading, i.e., improve catalyst stability, increase carbon capture, and decrease hydrogen consumption.

It is also observed that for stage 3 torrefaction and single stage fast pyrolysis experiments operating at pyrolysis conditions, the area profile of the non-condensable gases is nearly a straight line, i.e., the area of non-condensable gases sampled at different times during the feeding have similar GC-TCD area (the areas are within 5% of one another). This supports the assumption that at pyrolysis conditions, no further

significant decomposition of biomass occurs as it resides inside the reactor after the first few seconds. For example, Figure 5.1 shows the area profile of non-condensable gases observed during fast pyrolysis of oak for a total feeding time of 10 minutes. Similar behavior is observed in case of stage 3 thermal treatment as well.

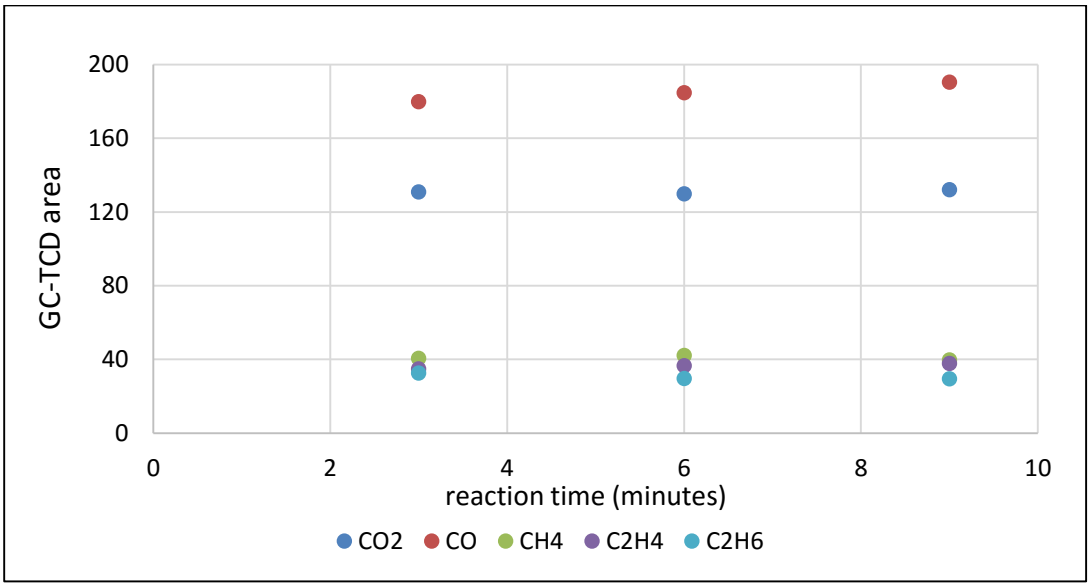

Figure 5.1: GC-TCD area of non-condensable gases sampled at different reaction times during fast pyrolysis of oak

5.1 Stage 3 Torrefaction

Similar to stage 1 thermal treatment, multiple batch runs of stage 2 torrefaction are carried out to obtain stage 2 solid residue for stage 3 experiments. The carbon content in the solid residue is measured after each batch experiment to ensure the carbon contents are similar before mixing the stage 2 solid obtained from different batch experiments.

Table 5.1 shows the overall mass balance for a single stage 3 torrefaction experiment. About 95.6% of the feed is recovered in the products.

Stage 2 solid residue (feed)	5.0 gm	100%
Char	2.9 gm	58.0%
Stage 3 liquid product	1.2 gm	24.0%
Non-condensable gases	0.68 gm	13.6%
Unaccounted mass	0.22 gm	4.4%

Table 5.1: Mass balance for stage 3 thermal treatment

One of the major challenges in analyzing the stage 3 liquid product is its low liquid yield. Also, in the case of stage 3, the condensate tends to adhere to the walls of the traps rather than pooling at the bottom. Therefore, a known amount of solvent (ethanol) is used to recover the liquid on the walls of the container from both the traps. A known concentration of stage 3 liquid in ethanol is obtained and analyzed using GC-FID and KF analyses. The carbon content of the liquid product is obtained from FID analysis since analyzing a diluted sample for carbon content in the elemental analyzer introduces significant error due to evaporation of solvent inside the furnace.

Figure 5.2 shows the selectivity of different compounds lumps present in the liquid collected from stage 3 thermal treatment. It is expected that at stage 3 conditions, the thermally stable lignin would decompose and produce a liquid stream comprising primarily phenolic species. Interestingly, levoglucosan which is derived from cellulose is the major organic product in the liquid stream rather than phenolic species, showing that at current stage 2 conditions, cellulose decomposition is largely incomplete. This result strongly suggests modifying stage 2 conditions to either increase cellulose decomposition (although more lignin decomposition will also occur), or to shift cellulose decomposition to stage 3.

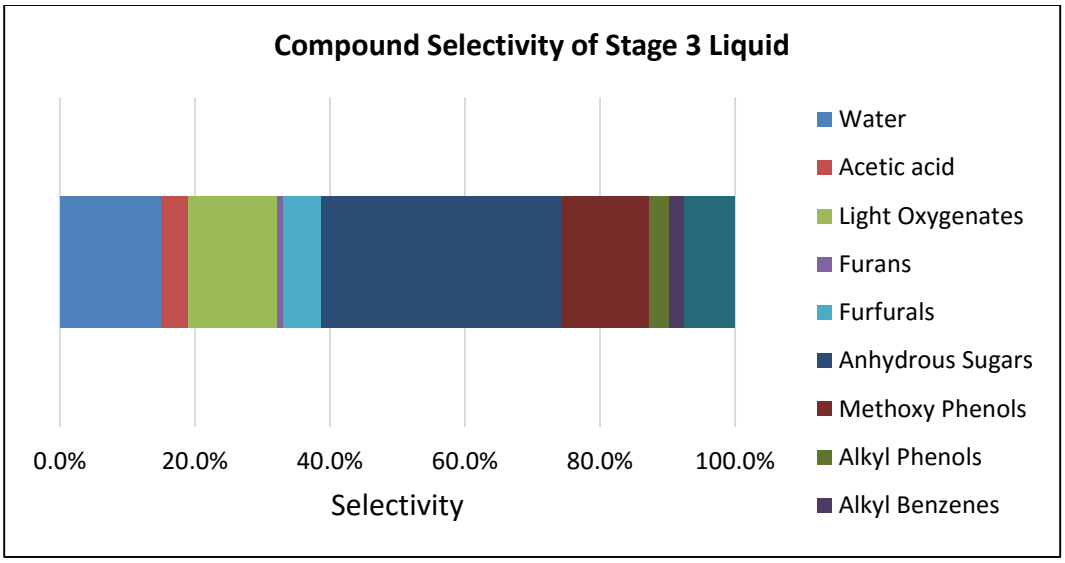

Figure 5.2: Mass selectivity of compounds present in stage 3 liquid product separated by compound groups

The carbon content measured in the condensed liquid product from stage 3 with respect to oak is shown in figure 5.2 and sums to 32.1 mg of carbon/gram of oak.

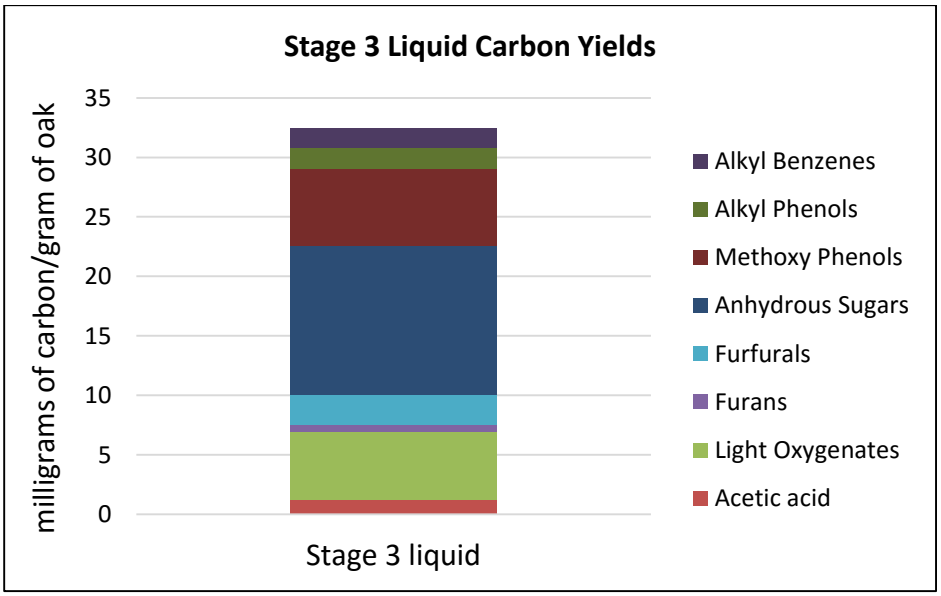

Figure 5.3: Stage 3 liquid carbon yields separated by compound groups with reference to raw oak biomass

5.2 Fast Pyrolysis of Oak

Fast pyrolysis of oak is used as a base case in order to compare the product yields with those obtained in the multi-stage torrefaction scenario.

Table 5.2 shows the overall mass balance for single step fast pyrolysis. About 95.6% of the raw oak is recovered in the products.

Oak fed to the reactor	6.2 gm	100%
Char	0.7 gm	11.3%
Bio-oil	3.8 gm	61.3%
Non-condensable gases	1.3 gm	21.0%
Unaccounted mass	0.4 gm	6.4%

Table 5.2: Mass balance for fast pyrolysis of oak

As mentioned previously, the unaccounted mass could be due to the non-condensation of vapors in the traps, as well as random error in the feed measurement due to the accuracy of feeder scale

Figure 5.3 shows the selectivity of different compounds lumps present in the bio-oil collected from fast pyrolysis oak. The bio-oil is a complex mixture of hundreds of compounds with no major compound/compound group and this is again reinstated in Figure 5.3. This poses serious challenges during catalytic upgrading as no one catalyst cannot be optimized to convert this complex mixture.

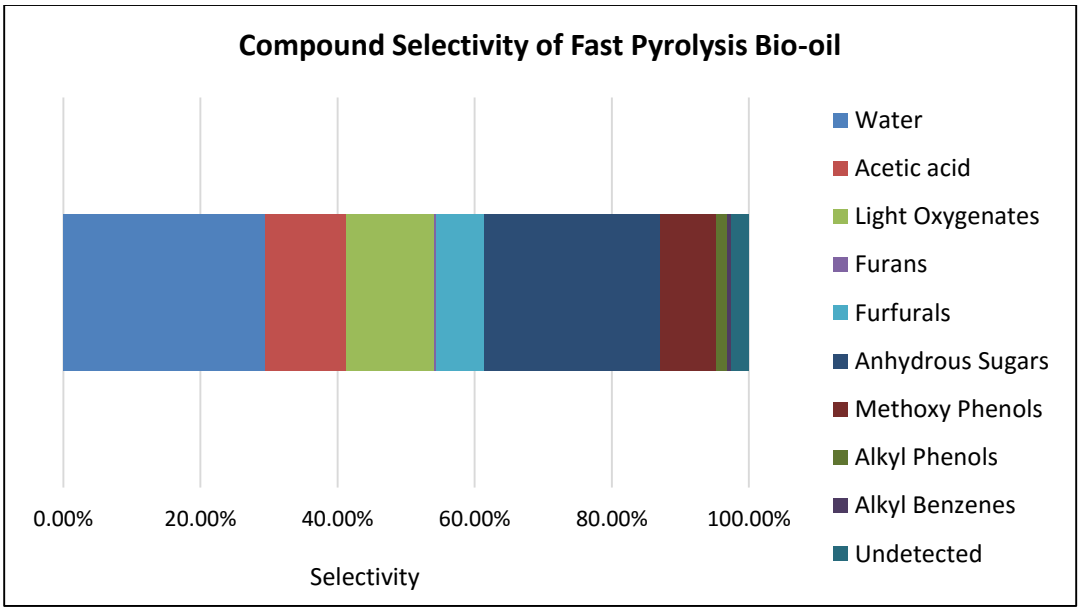

Figure 5.4: Mass selectivity of compounds present in fast pyrolysis bio-oil separated by compound groups

The carbon content measured in the condensed bio-oil from fast pyrolysis is shown in figure 5.4 and sums to 210 mg of carbon/gram of oak.

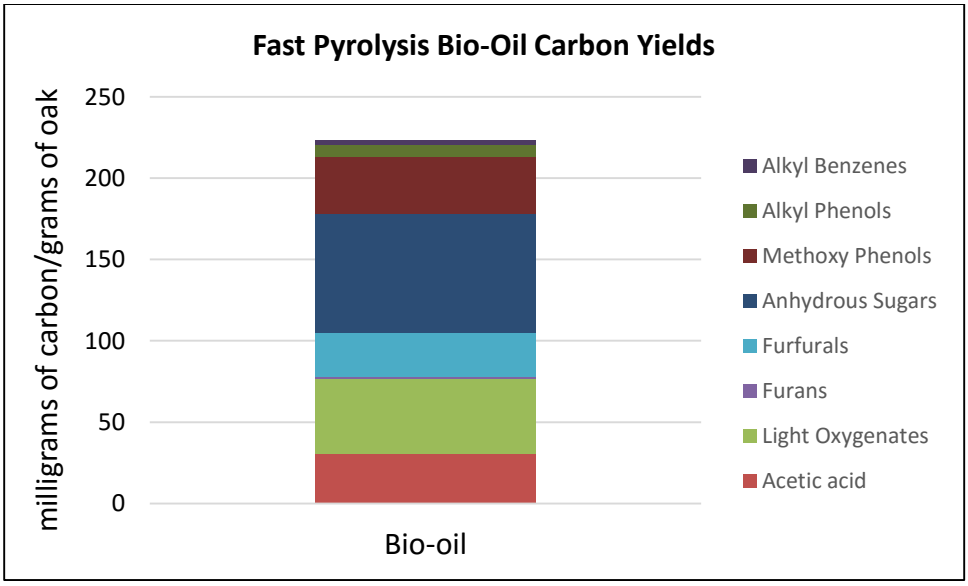

Figure 5.5: Carbon yields of fast pyrolysis bio-oil separated by compound groups

Chapter 6: Comparison of Multi-Stage Torrefaction with Single Step Fast Pyrolysis

The following sections give detailed mass balance and carbon balance for each stage and compares the cumulative yields from multi-stage thermal treatment with single-step fast pyrolysis by assuming 100 kg raw oak biomass is available initially.

6.1 Mass Balance

	Stage 1 torrefaction	Stage 2 torrefaction	Stage 3 torrefaction	Cumulative multi-stage torrefaction	Single step fast pyrolysis
Feed	100 kg	69.7 kg	31.6 kg	100 kg	100 kg
Solid product	69.7 kg	31.6 kg	18.3 kg	18.3 kg	11.3 kg
Liquid product	25.2 kg	28.7 kg	7.6 kg	61.5 kg	61.3 kg
Non-condensable gases	4.1 kg	5.7 kg	4.3 kg	14.1 kg	21.0 kg
Unaccounted mass	1.0 kg	3.6 kg	1.4 kg	6.1 kg	6.4 kg

Table 6.1: Mass balance for each individual stage and comparison of cumulative mass of products obtained from multi-stage torrefaction with single step fast pyrolysis of oak biomass

Initially, it is assumed that 100 kg of oak biomass is the starting quantity for each of the two scenarios. Table 6.1 presents product yield from each stage and compares the cumulative yields of three stage thermal treatment with single step fast pyrolysis. The total liquid product yield from both the routes is approximately the same but the total organic yield is higher in the case of fast pyrolysis due to higher water content from three stage thermal treatment. The total organic yield (total liquid product

minus total water content) from fast pyrolysis is 43.3% compared to 38 % from multi-stage thermal treatment.

6.2 Carbon Balance

The carbon content in the feed and the solid product is obtained by elemental analysis, carbon in non-condensable gases is quantified by Carle-GC and carbon content in liquid product is obtained from GC-FID analysis. Table 6.2 presents the carbon balance for the multi-stage scenario and compares it with single step fast pyrolysis.

	Kilograms of Carbon				
	Stage 1 torrefaction	Stage 2 torrefaction	Stage 3 torrefaction	Cumulative multi-stage torrefaction	Single Step fast pyrolysis
Feed	46.2	36.2	21.4	46.2	46.2
Solid product	36.2	21.4	15.2	15.2	9.8
Liquid product	5.2	9.1	3.2	17.5	21.0
Non-condensable gases	1.2	1.8	1.8	4.8	9.1
Unaccounted carbon	3.6	3.9	1.2	8.7	6.3

Table 6.2: Carbon balance for each individual stage and comparison of carbon mass in the products obtained from multi-stage torrefaction with single step fast pyrolysis of oak biomass

As discussed in earlier sections, the carbon unaccounted for in both the scenarios is primarily attributed to presence of oligomers in the liquid sample which is

undetected by GC analysis (either retained on the column or elutes at very long time) and therefore are not quantified by the GC-FID. Another significant factor could be the carbon lost in the unaccounted mass, i.e., 6.1% of oak is not recovered in any of the products and some part of the carbon is certainly lost in this unrecovered mass. Moreover, most the unidentified peak area in case of all the stages is observed at longer retention times in a GC chromatogram, where mainly methoxy phenols and furfurals are evolved and they have higher carbon to oxygen ratio (>2:1) compared to the light oxygenates (carbon to oxygen ratio of ≤ 1 for most of the compounds) observed at lower retention times.

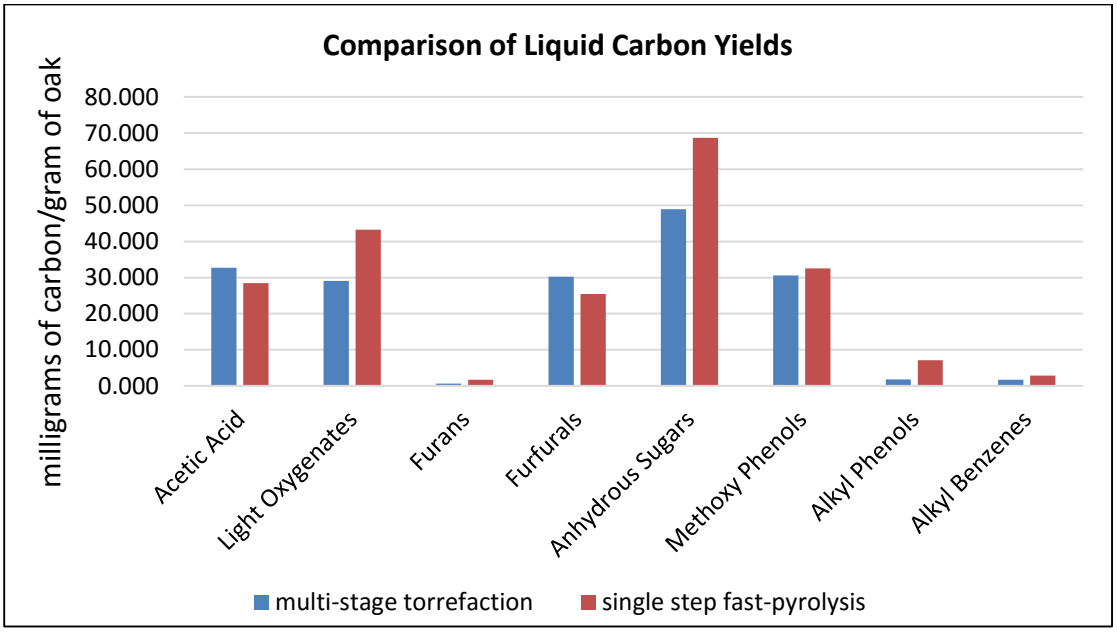

Figure 6.1: Comparison of liquid carbon yields between multi-stage thermal treatment and single step fast pyrolysis separated by compound groups

The observed lower total carbon yields from multiple stage torrefaction compared to the single step fast pyrolysis (especially in case levoglucosan as shown in Figure 6.2) is attributed to the increased thermal stability of biomass due to repolymerization and condensation reactions during stages 1 & 2 that are not kinetically

favored in case of fast pyrolysis. Zheng et al. noticed increase in peak area of the signal on the FTIR spectra at 1160 ppm which is assigned to C-O-C asymmetric vibration and this is as a result of crosslinking of cellulose during torrefaction (27). The mechanism for the effect of torrefaction on cellulose pyrolysis as reported in the literature is shown Figure 6.3 (27-29). In the case of direct fast pyrolysis of cellulose, initially active cellulose species are formed which subsequently decompose to sugar derived compounds (mainly levoglucosan). The levoglucosan can undergo further decomposition to form bio-oil, char and non-condensable gases. However, in the case of pyrolysis of torrefied cellulose, crosslinking of active cellulose unit occurs during torrefaction and this results in increased char yields during pyrolysis. Wen et al. (30) observed similar crosslinking behavior in the case of lignin where the ß-O-4 bonds have disappeared during torrefaction and increased aromatic C-C bonds are observed within lignin. These new refractory bonds have much higher dissociation enthalpies, and may not dissociate at typical fast pyrolysis temperatures, leading to enhanced char formation and corresponding loss of organic vapor yield.

The increase in char yields from multi-stage thermal treatment as reported in Table 7.1 could be due to crosslinking and charring of cellulose and lignin units. The crosslinking of cellulose units is further confirmed by the increase in char yields (Table 6.1) and decrease in levoglucosan yield (Figure 6.2) (Levoglucosan is a major cellulose decomposition product (31)) from multi-stage fractionation. Moreover, the decrease in yields of non-condensables and light oxygenates is also due to crosslinking of cellulose units as light oxygenates are obtained from cellulose decomposition whereas the non-condensables are obtained from levoglucosan decomposition (32).

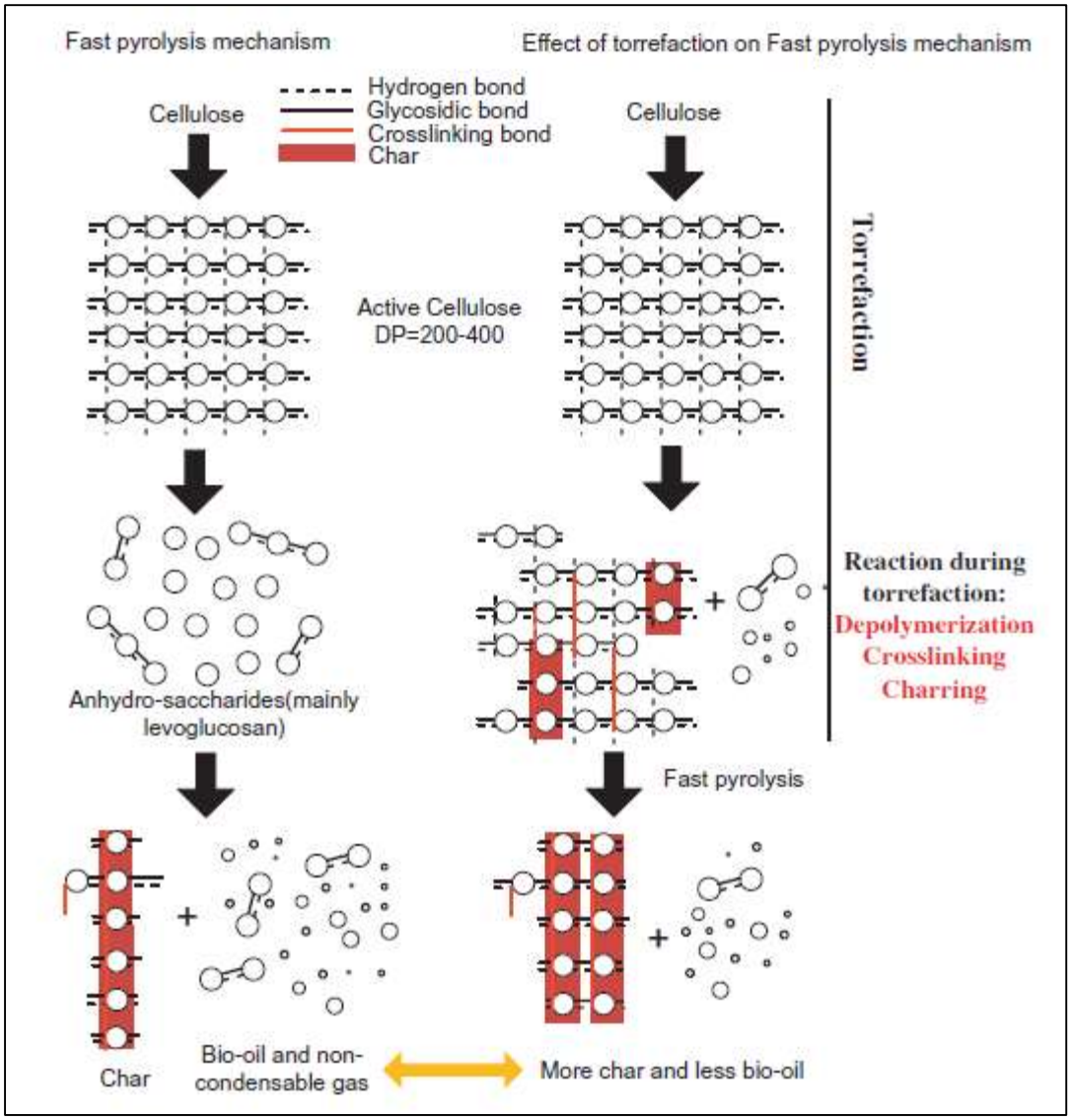

Figure 6.2: Effect of torrefaction on fast pyrolysis mechanism of cellulose

6.3 Discussion

The following sections lists two possible ways of improving the liquid carbon yield from staged fractionation and reducing the char yields.

6.3.1 Optimizing Process Conditions

The overall yield of char from multi-stage thermal treatment is higher compared to fast pyrolysis, as the extended heating time would lead to the solid becoming more

refractory and also due to repolymerization and condensation reactions happening during the stages 1 & 2. This increase in char formation coupled with decrease in the carbon yields from multi-stage thermal treatment could potentially be decreased by optimizing the process conditions for the first two stages. The optimal stage 1 conditions should achieve nearly complete degradation of the hemicellulose with minimal lignin and cellulose degradation while optimal stage 2 conditions should achieve thermal separation of cellulose- and lignin- derived products (e.g. levoglucosan and methoxy phenols) . Characterizing the stage 1 and stage 2 solid products for hemicellulose, cellulose and lignin contents and comparing their respective content in raw oak could enable more accurate determination of optimum residence time at different temperatures. Analytical pyrolysis studies on the pyroprobe can be carried out varying the process conditions such as time and temperature and processing it up to larger scale unit.

6.3.2 Improving the Efficiency of Condensers

A major part of the unaccounted mass is attributed to the non-condensation of vapors in the condensers. Therefore, it is necessary to improve the contact time of the vapors in the traps. This can be done by lowering the nitrogen carrier gas flowrate. However, that change would lead to longer residence time of the vapors inside the reactor and increased secondary reactions. Further, one can use glass beads to increase the contact time of the vapors inside the traps but recovering liquid on the glass beads would be problematic. Another alternative is to connect a third condenser in series with the current two and maintain it at ice water temperature. It is also noticed that, due to the extremely low temperature of liquid nitrogen, the vapors are condensed soon after

entering the traps and this leads to condensation on the walls of the traps. Therefore, having a second ice water condenser before the liquid nitrogen trap may help in avoiding the condensation on the walls of the trap as well as increase the residence time of the vapors inside the traps.

References

1. Tu Nguyet Pham, Dachuan Shi, Daniel E. Resasco. Evaluating strategies for catalytic upgrading of pyrolysis oil in liquid phase. Applied Catalysis B: Environmental 145 (2014) 10– 23.
2. Wenjia Jin, Kaushlendra Singh and John Zondlo. Pyrolysis Kinetics of Physical Components of Wood and Wood-Polymers Using Isoconversion Method. Agriculture 2013, 3, 12-32; doi: 10.3390/agriculture3010012.
3. Ragauskas, A.J., Williams, C.K., Davison, B.H., Britovsek, G., Cairney, J., Eckert, C.A., Frederick Jr., W.J., Hallett, J.P., Leak, D.J., Liotta, C.L., Mielenz, J.R., Murphy, R., Templer, R., Tschaplinski, T., 2006. The path forward for biofuels and biomaterials. Science 311, 484–489.
4. Arias BR, CG Pevida, JD Fermoso, MG Plaza, FG Rubiera, and JJ Pis Martinez (2008) "Influence of Torrefaction on the Grindability and Reactivity of Woody Biomass," Fuel Processing Technology, 89:2, pp. 169–175.
5. Paul de Wild, thesis, Biomass for chemicals, 2008.
6. M.J.C. van der Stelt, H. Gerhauser, J.H.A. Kiel, K.J. Ptasinski. Biomass upgrading by torrefaction for the production of biofuels: A review. Biomass and bioenergy 35 (2011) 3748-3762.
7. Prins, M.J., Ptasinski, K.J., Janssen, F.J.J.G., 2006b. Torrefaction of wood. Part 2: Analysis of products. J. Anal. Appl. Pyrol. 77, 35–40.
8. Chen WH, Kuo PC. A study on torrefaction of various biomass materials and its impact on lignocellulosic structure simulated by a thermogravimetry. Energy 2010, 35, 2580-86.

9. A.V. Bridgwater. Review of fast pyrolysis of biomass and product upgrading. Biomass and Bioenergy 38(2012) 68-94.
10. Meier, D., Faix, O., 1999. State of the art of applied fast pyrolysis of lignocellulosic materials: a review. Bioresource Technology 68, 71–77.
11. Mohan, D., Pittman, C.U., Steele, P.H., 2006. Pyrolysis of wood/biomass for bio-oil: a critical review. Energy Fuels 20, 848–889.
12. Lu Qiang, Li Wen-Zhi, Zhu Xi-Feng. Overview of fuel properties of biomass fast pyrolysis oils. Energy Conversion and Management 50 (2009) 1376–1383
13. Zhang Qi, Chang Jie, Wang Tiejun, Xu Ying. Review of biomass pyrolysis oil properties and upgrading research. Energy Conversion and Management 48 (2007) 87–92.
14. Prins, M.J., Ptasinski, K.J., Janssen, F.J.J.G., 2006a. Torrefaction of wood. Part 1: Weight loss kinetics. J. Anal. Appl. Pyrol. 77, 28–34.
15. Chen, D., Zheng, Z., Fu, K., Zeng, Z., Wang, J. Torrefaction of biomass stalk and its effect on the yield and quality of pyrolysis products. Fuel, 2015, 159.
16. Ren, S., Lei, H., Wang, L., Bu, Q., Chen, S., Wu, J., Julson, J., Ruan, R. The effects of torrefaction on compositions of bio-oil and syngas from biomass pyrolysis by microwave heating. Bioresource Technology 2013, 135, 659−64
17. Anqing Zheng, Zengli Zhao, Sheng Chang, Zhen Huang, Fang He, and Haibin Li. Effect of Torrefaction Temperature on Product Distribution from Two-Staged Pyrolysis of Biomass. Energy Fuels, 2012, 26, 2968-2974.
18. Meng, J., Park, J., Tilotta, D., Park, S., 2012. The effect of torrefaction on the chemistry of fast pyrolysis bio-oil. Bioresource Technology, 11, 439–446.

19. J.J. Chew, V. Doshi. Recent advances in biomass pretreatment – Torrefaction fundamentals and technology.
20. Christopher water, Thesis, (2016), Norman OK.
21. D. E. Resasco, What Should We Demand from the Catalysts Responsible for Upgrading Biomass Pyrolysis Oil? J. Phys. Chem. Lett. 2, 2294–2295 (2011).
22. O. Faix, D. Meier, I. Fortmann, Thermal degradation products of wood. Gas chromatographic separation and mass spectrometric characterization of monomeric lignin-derived products. Holz als Roh-und Werkstoff (1990).
23. O. Faix, I. Fortmann, J. Bremer, D. Meier, Thermal degradation products of wood: Gas chromatographic separation and mass spectrometric characterization of polysaccharide derived products. Holz als Roh-und Werkstoff (1991).
24. P. J. Dauenhauer, A. D. Paulsen, M. S. Mettler. The Role of Sample Dimension and Temperature in Cellulose Pyrolysis. Energy & Fuels. 27, 2126–2134 (2013).
25. P. R. Patwardhan, R. C. Brown, B. H. Shanks, Understanding the Fast Pyrolysis of Lignin. ChemSusChem. 4, 1629–1636 (2011).
26. P. R. Patwardhan, D. L. Dalluge, B. H. Shanks, Distinguishing primary and secondary reactions of cellulose pyrolysis. Bioresource technology (2011), doi:10.1016/j.biortech.2011.02.018.
27. Anqing Zheng, Zengli Zhao, Sheng Chang, Zhen Huang, Fang He, and Haibin Li. Effect of torrefaction on structure and fast pyrolysis behavior of corncobs. Bioresource Technology 128 (2013) 370–377.

28. Chaiwat, W., Hasegawa, I., Kori, J., Mae, K., 2008. Examination of degree of crosslinking for cellulose precursors pretreated with acid/hot water at low temperature. Ind. Eng. Chem. Res. 47 (16), 5948–5956.
29. Lin, Y.C., Cho, J., Tompsett, G.A., Westmoreland, P.R., Huber, G.W., 2009. Kinetics and mechanism of cellulose pyrolysis. J. Phys. Chem. C 113 (46), 20097–20107.
30. J.-L. Wen, S.-L. Sun, T.-Q. Yuan, F. Xu, R.-C. Sun, Understanding the chemical and structural transformations of lignin macromolecule during torrefaction. APPLIED ENERGY. 121, 1–9 (2014).
31. P. R. Patwardhan, D. L. Dalluge, B. H. Shanks, Distinguishing primary and secondary reactions of cellulose pyrolysis. Bioresource technology (2011), doi:10.1016/j.biortech.2011.02.018
32. X. L. Zhang, W. H. Yang, C. Q. Dong, Levoglucosan formation mechanisms during cellulose pyrolysis. Journal of Analytical and Applied Pyrolysis. 104, 19–27 (2013).
33. W. J. Grigsby, G. Varhegyi, C. Di Blasi, Thermogravimetric analysis and devolatilization kinetics of wood. *Ind. Eng. Chem. Res.* (2002), doi:10.1016/j.carbpol.2014.01.086.
34. W. H. Chen, P. C. Kuo, Torrefaction and co-torrefaction characterization of hemicellulose, cellulose and lignin as well as torrefaction of some basic constituents in biomass. *Energy* (2011), doi:10.1016/j.energy.2010.12.036.

35. W. H. Chen, P. C. Kuo, Isothermal torrefaction kinetics of hemicellulose, cellulose, lignin and xylan using thermogravimetric analysis. *Energy* (2011), doi:10.1016/j.energy.2011.09.022.
36. P. A. Horne, P. T. Williams, Influence of temperature on the products from the flash pyrolysis of biomass. Fuel (1996).

Appendix A: Supplementary Figures and Tables

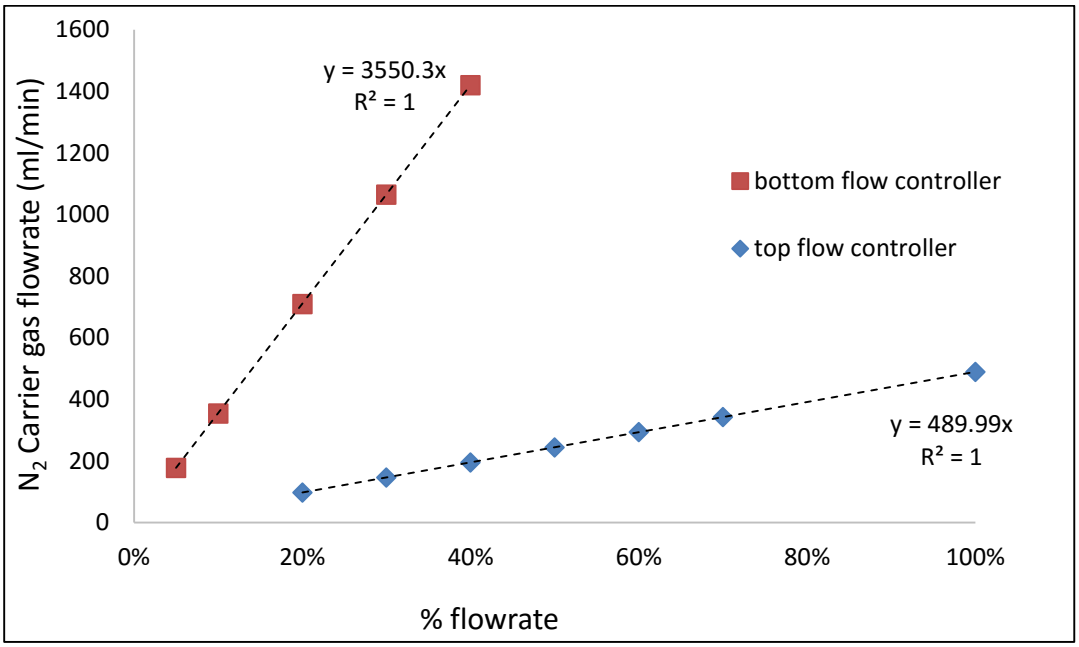

Figure A1: Flowrate calibration of nitrogen carrier gas for the two flow controllers with wet test meter

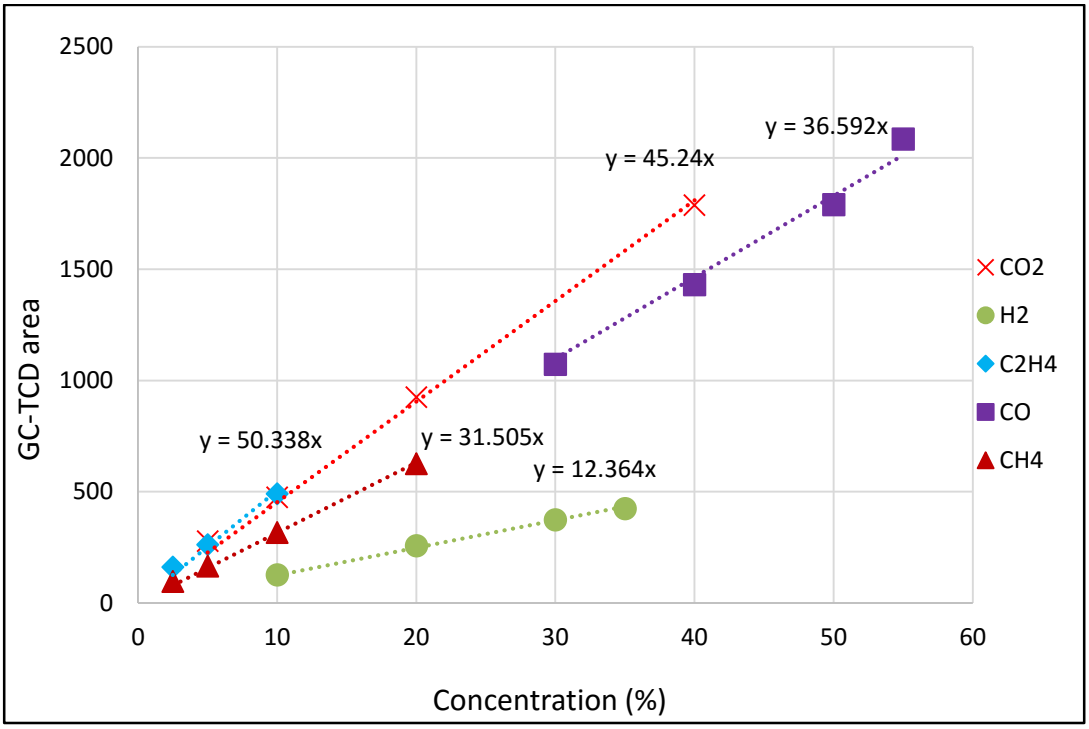

Figure A2: Calibration curve of various standard gases with Carle-GC

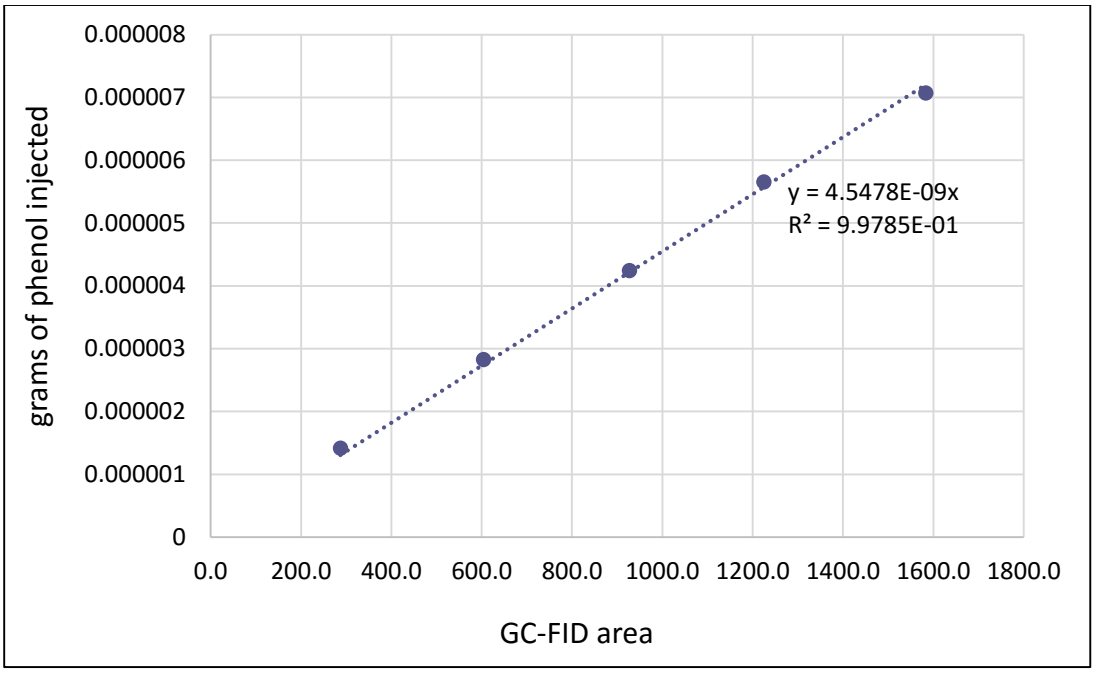

Figure A3: Calibration curve of phenol with GC-FID

Name of the compound	Compound group	ECN	Response factor (grams/area)
Acetic acid	Acetic Acid	0.6845	2.046E-08
2-Propenal	Light Oxygenates	1.9031	6.868E-09
Propanal-2-one	Light Oxygenates	1.9031	8.830E-09
Butanal	Light Oxygenates	2.8876	5.820E-09
1-Penten-3-one	Light Oxygenates	3.8720	5.063E-09
2,3-Butanedione	Light Oxygenates	1.8373	1.092E-08
3-Pentanone	Light Oxygenates	3.8720	5.184E-09
2-Butanone	Light Oxygenates	2.8876	5.820E-09
Hydroxyacetaldehyde	Light Oxygenates	0.4117	3.402E-08
2-Butenal (cis or trans)	Light Oxygenates	2.8876	5.658E-09
2-Hydroxypropanal	Light Oxygenates	1.3166	1.312E-08
Hydroxypropanone	Light Oxygenates	1.3962	1.237E-08
2-Propenoic acid methyl ester	Light Oxygenates	2.4949	8.046E-09
1-Hydroxy-2-butanone	Light Oxygenates	2.3806	8.628E-09
3-Hydroxypropanal	Light Oxygenates	1.3962	1.237E-08
2-Hydroxy-3-oxobutanal	Light Oxygenates	1.2508	1.903E-08
1-Acetyloxypropane-2-one	Light Oxygenates	2.4291	1.115E-08
2-Hydroxy-butanedial	Light Oxygenates	1.2508	1.903E-08
Butanedial	Light Oxygenates	1.8373	1.092E-08
2,3-Dihydroxyhex-1-ene-4-one	Light Oxygenates	3.6834	8.238E-09

Furan	Furans	3.7662	4.214E-09
2-Methylfuran	Furans	4.6105	4.151E-09
2-Acetylfuran	Furans	4.6849	5.480E-09
2,3-Dihydro Furan	Furans	3.8520	4.241E-09
(2H)-Furan-3-one	Furans	1.3829	1.418E-08
2-Furaldehyde	Furfurals	2.3674	9.465E-09
2-Furfuryl alcohol	Furfurals	2.9107	7.858E-09
5-Methyl-2-furaldehyde	Furfurals	3.3518	7.660E-09
(5H)-Furan-2-one	Furfurals	1.3829	1.418E-08
Dihydro-methyl-furanone	Furfurals	2.3674	9.662E-09
2-Hydroxy-1-methyl-1-cyclopentene-3-one	Furfurals	4.2699	6.122E-09
Methyl-butyraldehyde derivative	Furfurals	3.8720	5.184E-09
gamma-Lactone derivative	Furfurals	0.9902	2.027E-08
gamma-Butyrolactone	Furfurals	0.9902	2.027E-08
5-Hydroxymethyl-2-furaldehyde	Furfurals	2.8449	1.034E-08
4-Cyclopentene-1,3-dione	Furfurals	2.8218	8.271E-09
2-Furoic acid methyl ester	Furfurals	2.9591	9.938E-09
OH-methyl-dihydropyranone	Furfurals	4.2699	6.997E-09
4-Hydroxy-5,6-dihydro-(2H)-pyran-2-one	Furfurals	3.2855	8.099E-09
3-Hydroxy-2-methyl-pyran-4-one	Furfurals	2.7653	1.063E-08
Methyl-dihydro-(2H)-pyran-2-one	Furfurals	3.3518	7.799E-09
Levoglucosan	Levoglucosan	1.1378	3.323E-08
1,4:3,6-Dianhydro-glucopyranose	Anhydrous Sugars	0.8062	4.169E-08
1,6-Anhydro-beta-D-mannopyranose	Anhydrous Sugars	1.1378	3.323E-08
1,5-Anhydro-beta-D-xylofuranose	Anhydrous Sugars	0.7399	4.164E-08
Anhydrosugar: unknown	Anhydrous Sugars	1.1378	3.323E-08
Toluene	Alkyl Benzenes	6.4936	3.307E-09
Phenol	Alkyl Phenols	4.8243	4.548E-09
Styrene	Alkyl Benzenes	7.4780	3.246E-09
Benzene, ethyl-	Alkyl Benzenes	7.4780	3.308E-09
Benzene, 1,2-dimethyl-	Alkyl Benzenes	7.3378	3.372E-09
Benzaldehyde	Alkyl Benzenes	5.5836	4.431E-09
Anisole	Alkyl Benzenes	5.6302	4.477E-09
Benzylalcohol	Alkyl Benzenes	6.1268	4.114E-09
o-Cresol	Alkyl Phenols	5.6685	4.447E-09
Catechol	Alkyl Phenols	3.9992	6.420E-09
Acetophenone	Alkyl Phenols	6.5680	4.264E-09
Phenol, 4-vinyl-	Alkyl Phenols	6.6530	4.210E-09
Phenol, 2,6-dimethyl-	Alkyl Phenols	6.5128	4.372E-09
Phenol, 2-ethyl-	Alkyl Phenols	6.6530	4.280E-09

Benzaldehyde, 4-hydroxy-	Alkyl Benzenes	4.7585	5.984E-09
Guaiacol	Methoxy Phenols	4.8052	6.023E-09
Catechol, 3-methyl-	Alkyl Phenols	4.8434	5.975E-09
Phenol, 4-allyl-	Alkyl Phenols	7.6374	4.095E-09
Phenol, 4-propenyl-	Alkyl Phenols	7.6374	4.095E-09
Anisole, 2,4-/2,5-dimethyl-	Alkyl Benzenes	7.3187	4.337E-09
Phenol, 2-propyl-	Alkyl Phenols	7.6374	4.156E-09
Guaiacol, 3-methyl-	Methoxy Phenols	5.6494	5.701E-09
Guaiacol, 4-vinyl-	Methoxy Phenols	6.6339	5.278E-09
Guaiacol, 3-ethyl	Methoxy Phenols	6.6339	5.348E-09
Vanillin	Methoxy Phenols	4.7394	7.486E-09
Syringol	Methoxy Phenols	4.7860	7.510E-09
Eugenol	Methoxy Phenols	7.6183	5.024E-09
Isoeugenol	Methoxy Phenols	7.6183	5.024E-09
Guaiacol, 4-propyl-	Methoxy Phenols	7.6183	5.086E-09
Homovanillin	Methoxy Phenols	5.5836	6.939E-09
Acetoguaiacone	Methoxy Phenols	5.7238	6.769E-09
Syringol, 4-methyl-	Methoxy Phenols	5.6303	6.964E-09
Vanillic acid	Methoxy Phenols	4.5052	8.704E-09
Guaiacol, 4-(oxy-allyl)-	Methoxy Phenols	6.7083	6.193E-09
Coniferaldehyde	Methoxy Phenols	6.5681	6.325E-09
Syringol, 4-vinyl-	Methoxy Phenols	6.6147	6.351E-09
Guaiacyl acetone	Methoxy Phenols	6.5681	6.396E-09
Propioguaiacone	Methoxy Phenols	6.7083	6.263E-09
Coniferyl alcohol	Methoxy Phenols	7.1113	5.908E-09
Syringol, 3-ethyl-	Methoxy Phenols	6.6147	6.422E-09
Dihydroconiferyl alcohol	Methoxy Phenols	7.1113	5.973E-09
Syringaldehyde	Methoxy Phenols	4.7203	8.999E-09
Syringol, 4-allyl-	Methoxy Phenols	7.5992	5.959E-09
Propioguaiacone, alpha-oxy-	Methoxy Phenols	5.6580	8.003E-09
Syringol, 4-propenyl-	Methoxy Phenols	7.5992	5.959E-09
Syringol, 4-propyl-	Methoxy Phenols	7.5992	6.020E-09
Homosyringaldehyde	Methoxy Phenols	5.7047	8.019E-09
Acetosyringone	Methoxy Phenols	5.7047	8.019E-09
Syringol, 4-(oxy-allyl)-	Methoxy Phenols	6.6892	7.327E-09
Sinapaldehyde	Methoxy Phenols	5.5645	8.725E-09
Syringyl acetone	Methoxy Phenols	6.5489	7.484E-09
Propiosyringone	Methoxy Phenols	6.6892	7.327E-09
Sinapyl alcohol	Methoxy Phenols	7.0922	6.911E-09
Propiosyringone, alpha-oxy-	Methoxy Phenols	5.6389	9.272E-09

Table A1: Effective carbon number, response factor and compound group of identified compounds in this study

Trial	Water content (wt. %)			
	Stage 1	Stage 2	Stage 3	Single step fast pyrolysis
1	51.0	37.8	15.5	29.8
2	50.6	37.1	14.8	29.1
3	49.3	38.1	14.7	29.3
Average	50.3	37.6	15.0	29.4

Table A2: Water content present in the liquid product obtained from three torrefaction stages and single step fast pyrolysis as quantified by Karl Fischer titration

gas	grams			
	Stage 1	Stage 2	Stage 3	Single step fast pyrolysis
CO_2	0.52	0.56	0.29	0.52
CO	0.10	0.24	0.27	0.54
CH_4	0	0	0.08	0.07
C_2H_4	0	0	0.02	0.09
C_2H_6	0	0	0.02	0.08

Table A3: Composition of non-condensable gases from different torrefaction stages and single step fast pyrolysis as quantified with Carle-GC

Compound group	Kilograms of compound/100 kg of raw oak biomass				
	Stage 1	Stage 2	Stage 3	Cumulative multi-stage	Single step fast pyrolysis
Water	12.66	9.63	1.14	23.42	18.00
Acetic Acid	5.81	2.04	0.30	8.16	6.79
Light Oxygenates	1.38	3.54	1.01	5.93	7.40
Furans	0.00	0.02	0.07	0.08	0.22
Furfurals	1.60	3.09	0.42	5.11	4.02
Anhydrous Sugars	1.01	7.15	2.72	10.89	14.78
Methoxy Phenols	1.26	2.40	0.98	4.63	4.70
Alkyl Phenols	0.00	0.02	0.22	0.24	0.94
Alkyl Benzenes	0.00	0.00	0.18	0.18	0.29
Undetected	1.43	0.82	0.57	2.81	4.15
Total	25.15	28.70	7.60	61.45	61.30

Table A4: Detailed liquid product distribution of the three stages of torrefaction and single step fast pyrolysis quantified by GC-FID and separated by compound groups

Compound group	Milligrams of carbon/gram of raw oak biomass				
	Stage 1	Stage 2	Stage 3	Cumulative multi-stage	Single step fast pyrolysis
Acetic Acid	23.25	8.18	1.24	32.67	28.43
Light Oxygenates	6.42	16.86	5.77	29.05	43.25
Furans	0.00	0.10	0.51	0.60	1.71
Furfurals	9.36	18.29	2.56	30.21	25.48
Anhydrous Sugars	4.50	31.97	12.46	48.94	68.67
Methoxy Phenols	8.38	15.63	6.54	30.55	32.51
Alkyl Phenols	0.00	0.12	1.69	1.81	7.07
Alkyl Benzenes	0.00	0.00	1.65	1.65	2.88
Total	51.92	91.15	32.42	175.48	209.99

Table A5: Carbon content in liquid product obtained from three stages of torrefaction and single step fast pyrolysis separated by compound groups and quantified by GC-FID

Appendix B: Stage 1 Torrefaction Sample Calculation

CO and CO_2 Quantification

Figure B1 shows the area profile (GC area vs. reaction time) of CO and CO_2 as a function of time, measured during stage 1 torrefaction from a gas sampled at regular intervals during a reaction and injected into Carle AGC.

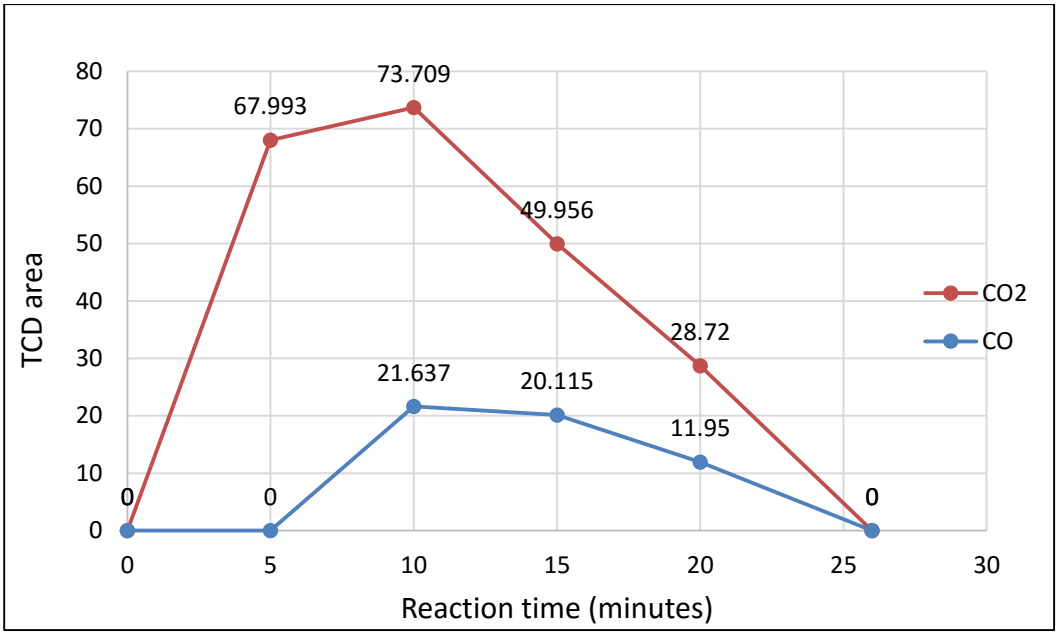

Figure B1: Area profile of CO and CO_2 for stage 1 torrefaction

The total area under the curve for each of CO and CO_2 curves is obtained by calculating the area under the curve between two successive points and finally summing all the areas. Average area is obtained by dividing the total area with the total reaction time, i.e., the time taken for the biomass to stop decomposing and producing vapors (time taken for biomass to drop below 200°C in the case of stage 1).

	0-5 min	5-10 min	10-15 min	15-20 min	20-27 min	Total
CO_2 Area	169.98	354.26	309.16	196.69	86.16	1116.25

Table B1: Area of CO_2 under the curve between two successive time intervals

	0-5 min	5-10 min	10-15 min	15-20 min	20-26 min	Total
CO Area	0	54.09	104.38	80.16	35.85	274.48

Table B2: Area of CO under the curve between two successive time intervals

- Total reaction time = 26 minutes
- Average effluent flowrate = 1032.16 ml/min
- Average CO_2 area = 1116.25/26 = 41.343
- Calibration curved of CO_2 is represented by the equation (refer figure A2)

Y = 42.278*X

Y= TCD area of CO_2

X = mole %

- Average CO_2 mole % = 41.343/42.278 = 0.978
- Mass of CO_2 assuming STP conditions = (1032.16*26/1000)*(0.978/100)*(44/22.4)

= 0.515 g

- Average CO area = 274.48/26 = 10.56
- Calibration curved of CO is represented by the equation (refer figure A2)

Y = 36.349*X

Y= TCD area of CO

X = mole %

- Average CO mole % = 10.56/36.349 = 0.29
- Mass of CO assuming STP conditions = (1032.16*26/1000)*(0.29/100)*(28/22.4)

= 0.097 g

- Total mass of non-condensable gases = 0.515+0.097 = 0.61 g

Mass Balance

- Total oak fed to the reactor = 15.5 g
- Total stage 1 residue collected = 10.8 g
- Total stage 1 liquid product collected = 3.9 g
- Mass of non-condensable gases computed using Carle GC = 0.61 g
- Total mass unaccounted for (by difference) = 0.19 g

Organic Compound Quantification from FID Analysis

Since more than 50 organic compounds are identified in the stage 1 liquid product, the sample calculation for obtaining the grams of only one organic compound is outlined. The sample calculation for acetic acid is described here because it is one of the major compounds in stage 1 liquid product.

- Total FID area after integration = 28208.98
- Total FID area identified = 24488.99
- % of FID area identified = 24488.89/28208.98 = 86.81%

The remaining unidentified FID area is evenly distributed among all the compounds, i.e., the area of each compound is multiplied by a factor of (1/0.8681)

- FID area of acetic acid obtained by integration = 8762.06
- FID area of acetic acid after area correction = 8762.06*(1/0.8681) = 100093.05

Response factor of acetic acid is obtained by using a combination of phenol calibration curve and ECN model

- Response factor (grams/area) of acetic acid (refer table A1) = 2.046E-08 grams/area
- Grams of acetic acid in 1µL of solution injected into GC = 100093.05*2.046E-08

  = 0.207 mg

The 1µL solution injected into the GC is mixture of stage 1 liquid and ethyl alcohol (solvent). It is therefore necessary to determine how much of this injected solution is stage 1 liquid. A known amount of stage 1 liquid and ethyl alcohol is taken in a GC vial and 1µL of this solution is injected into GC

- Amount of stage 1 liquid in GC vial = 1.219 g
- Amount of ethanol in GC vial = 0.232 g
- Density of ethanol = 0.789 g/ml
- Density of stage 1 liquid = 1.14 g/ml

Density of stage 1 liquid is obtained by pipetting out known volume of liquid and measuring its weight. This procedure is followed multiple times and the average value is taken as the density of stage 1 liquid.

- Density of solution = $\frac{1.219+0.232}{\left(\frac{1.219}{1.14}\right)+\left(\frac{0.232}{0.789}\right)}$ = 1.064 g/ml
- Amount of the solution injected = 1µL * 1.064 g/ml = 1.064 mg
- Mass fraction of stage 1 liquid in GC vial = 1.219/ (1.219+0.232) = 0.84
- Amount of stage 1 liquid injected = 1.064*0.84 = 0.894 mg

Therefore, 0.207 mg of acetic acid that is obtained when 1µL of solution is injected is actually obtained from injecting 0.894 mg of stage 1 liquid.

- Grams of acetic acid in 1 g of stage 1 liquid injected = 0.207*1000*(1/0.894)

  = 0.231 g
- Grams of carbon from acetic acid in stage 1 liquid = 0.231 *12*2/60 = 0.0924 g

Similarly, the amount of other organic compounds and their respective carbon content in stage 1 liquid product is computed

- Total amount of all the organic compounds in 1 g of stage 1 liquid from FID analysis = 0.44 g
- Grams of water in stage 1 liquid = 0.50 g
- Mass of liquid product unaccounted for in 1 g of stage 1 liquid
  = 1-0.44-0.50 = 0.06 g (6%)
- Total amount of carbon in 1 g of stage 1 liquid from FID analysis = 0.206 g

Carbon Balance

While the amount of carbon in oak and stage 1 solid product can be obtained from elemental analysis, the amount of carbon in stage 1 liquid product can be obtained from either elemental analysis or FID analysis. The following table gives the CHO breakdown from elemental analysis.

Sample	% C	% H	% O
Oak	46.21	5.88	47.91
Stage 1 solid residue	25.82	8.33	65.85
Stage 1 liquid product	51.94	5367	42.39

Table B3: Elemental analysis of different materials involved in stage 1

Based on the carbon content in the feed and products obtained from various analyses, the following calculation shows how much of the carbon that is fed to the reactor is recovered in the products.

- Carbon content in oak = 15.5*0.462 = 7.156 g
- Carbon content in stage 1 solid residue = 10.8*0.519 = 5.609 g
- Carbon content in stage 1 liquid from EA = 3.9*0.258 = 0.997 g
- Carbon content in non-condensable gases = (0.515*12/44)+(0.097*12/28) = 0.182 g

- Carbon unaccounted for considering elemental analysis on liquid product = 0.368 g
- % of carbon unaccounted for considering elemental analysis on liquid product = 0.368/7.156 = 5.14%
- Total amount of carbon in stage 1 liquid from FID analysis = 0.795 g
- % of carbon unaccounted for considering FID analysis on liquid product = 7.96%